Inorganic Chemistry
Cite This: Inorg. Chem. XXXX, XXX, XXX−XXX
Article
pubs.acs.org/IC

Catalytic Hydrolysis of Phosphate Monoester by Supramolecular Phosphatases Formed from a Monoalkylated Dizinc(II) Complex, Cyclic Diimide Units, and Copper(II) in Two-Phase Solvent System

Akib Bin Rahman,[†] Hiroki Imafuku,[†] Yuya Miyazawa,[†] Ananda Kafle,[§] Hideki Sakai,[§] Yutaka Saga,[†] and Shin Aoki*[,†,∥,⊥]

[†]Faculty of Pharmaceutical Science, [§]Faculty of Science and Technology, [∥]Division of Medical-Science-Engineering Cooperation, Research Institute for Science and Technology, [⊥]Imaging Frontier Center, Research Institute for Science and Technology, Tokyo University of Science, 2641 Yamazaki, Noda, Chiba 278-8510, Japan

Supporting Information

ABSTRACT: Design and synthesis of enzyme mimic with programmed molecular interaction among several building blocks including metal complexes and metal chelators is of intellectual and practical significance. The preparation of artificial enzymes that mimic the natural enzymes such as hydrolases, phosphatases, etc. remains a great challenge in the field of supramolecular chemistry. Herein we report on the design and synthesis of asymmetric (nonsymmetric) supermolecules by the 2:2:2 self-assembly of an amphiphilic zinc(II)−cyclen complex containing a 2,2′-bipyridyl linker and one long alkyl chain (Zn_2L^3), barbital analogues, and Cu^{2+} as model compounds of an enzyme alkaline phosphatase that catalyzes the hydrolysis of phosphate monoesters such as mono(4-nitrophenyl)phosphate at neutral pH in two-phase solvent system ($H_2O/CHCl_3$) in pH 7.4 and 37 °C. Hydrolytic activity of these complexes was found to be catalytic, and their catalytic turnover numbers are 3−4. The mechanistic studies based on the UV/vis and emission spectra of the H_2O and $CHCl_3$ phases of the reaction mixtures suggest that the hydrophilicity/hydrophobicity balance of the supramolecular catalysts is an important factor for catalytic activity.

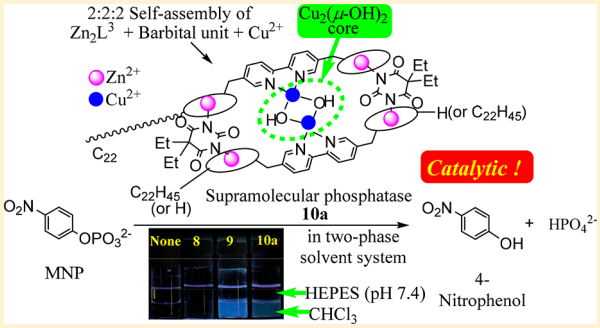

INTRODUCTION

The phosphorylation and dephosphorylation of proteins and enzymes are important processes in intracellular regulation. The dephosphorylation of phosphoserine and phosphothreonine residues in proteins, the reverse of phosphorylation, by protein kinase is catalyzed by protein phosphatases.[1] For example, alkaline phosphatases (APs) occur widely in nature and are found in many organisms from bacteria to human. The three-dimensional structure of AP indicates that APs are homodimeric enzymes and that each catalytic site contains three metal ions; that is, two Zn ions and one Mg ion are required, not for only catalytic activity for the hydrolysis of monoesters of phosphoric acid but also for transphosphorylation reactions that proceed in the presence of large concentrations of phosphorylation acceptors.[2] The active sites of phosphatases are similar in that they include dimetallic diamond-shaped cores containing two metal cations, which are coordinated by hydroxide ions and amino acids. Although chemical models for hydrolases such as phosphatases have been developed,[3,4] artificial compounds that catalyze the hydrolysis of phosphonic acid monoester such as mono(4-nitrophenyl)phosphate (MNP) are rare, because phosphate monoesters are less reactive than phosphate diesters and triesters.[4a,i,5]

Supramolecular strategies are useful for the construction of three-dimensional and well-defined structures that can be useful in molecular recognition, molecular sensing, molecular storage, electronic devices, and catalytic reactions.[6−8] In this context, we previously reported on the formation of a supramolecular complex **8** by the 2:2:2 assembly of dimeric zinc(II) (Zn^{2+}-cyclen) complexes containing a 2,2′-bipyridyl (bpy) linker **1** (Zn_2L^1), a dianion of barbital (Bar^{2-}) and its analogues (**4**), and a copper ion (Cu^{2+}) via 2:2 complexes of **1** with **4** (cyclen = 1,4,7,10-tetraazacyclododecane).[9,10] It was discovered that **8** possesses a $Cu_2(\mu\text{-}OH)_2$ core that is analogous to the active sites (Fe−Zn or Zn−Zn) of naturally occurring dinuclear metalloenzymes such as AP. In addition, these supramolecular complexes were found to accelerate the hydrolysis of MNP at a neutral pH in single-phase aqueous solution and in a two-phase solvent system ($CHCl_3$/50 mM 4-(2-hydroxyethyl)-1-piperazineethanesulfonic acid (HEPES)). Although **8** accelerates the hydrolysis of MNP, catalytic turnover was not observed, possibly because the hydrolytic activity of **8** is inhibited by HPO_4^{2-}, an MNP hydrolysis

Received: December 24, 2018

DOI: 10.1021/acs.inorgchem.8b03586
Inorg. Chem. XXXX, XXX, XXX−XXX

Scheme 1. Formation of the 2:2:2 Supermolecules 8, 9, and 10 from Zn_2L complexes (1−3), 5,5′-Diethylbarbital (Bar^{2-}) Derivatives (4a−f), and Cu^{2+} that Accelerate the Hydrolysis of MNP in a Single (H_2O) and a Two-Phase Solvent System ($CHCl_3/H_2O$)

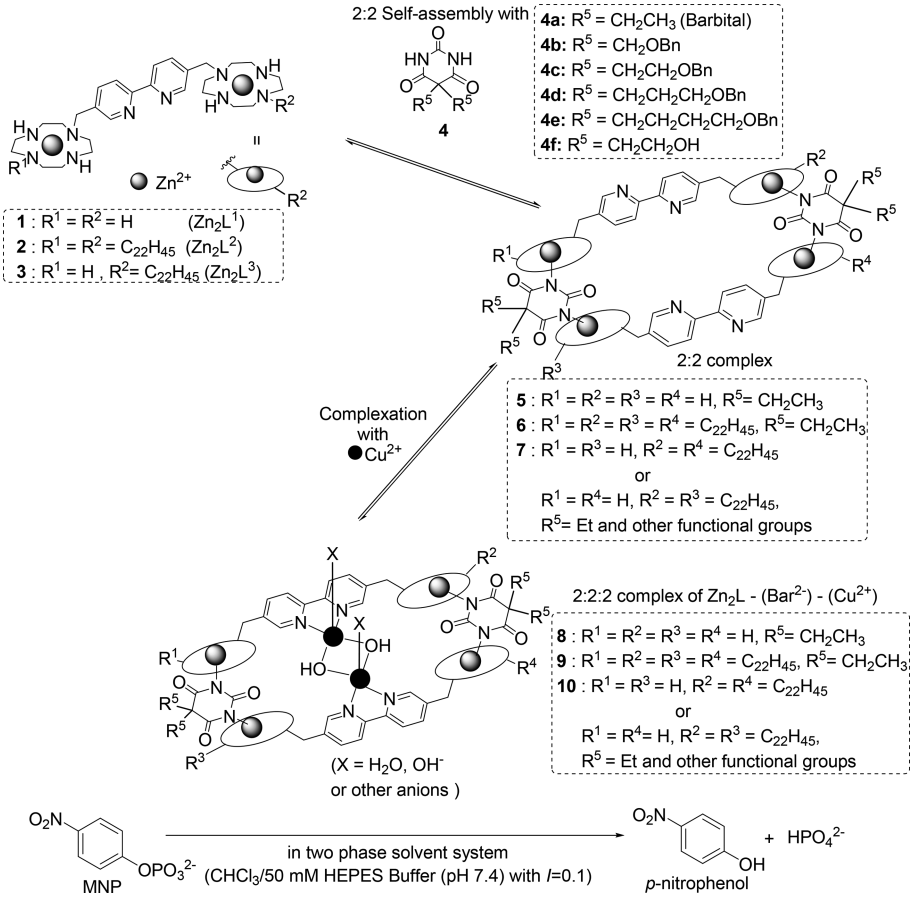

Scheme 2. Proposed Scheme of Hydrolysis of MNP by Artificial Phosphatases 10 in a Two-Phase Solvent System

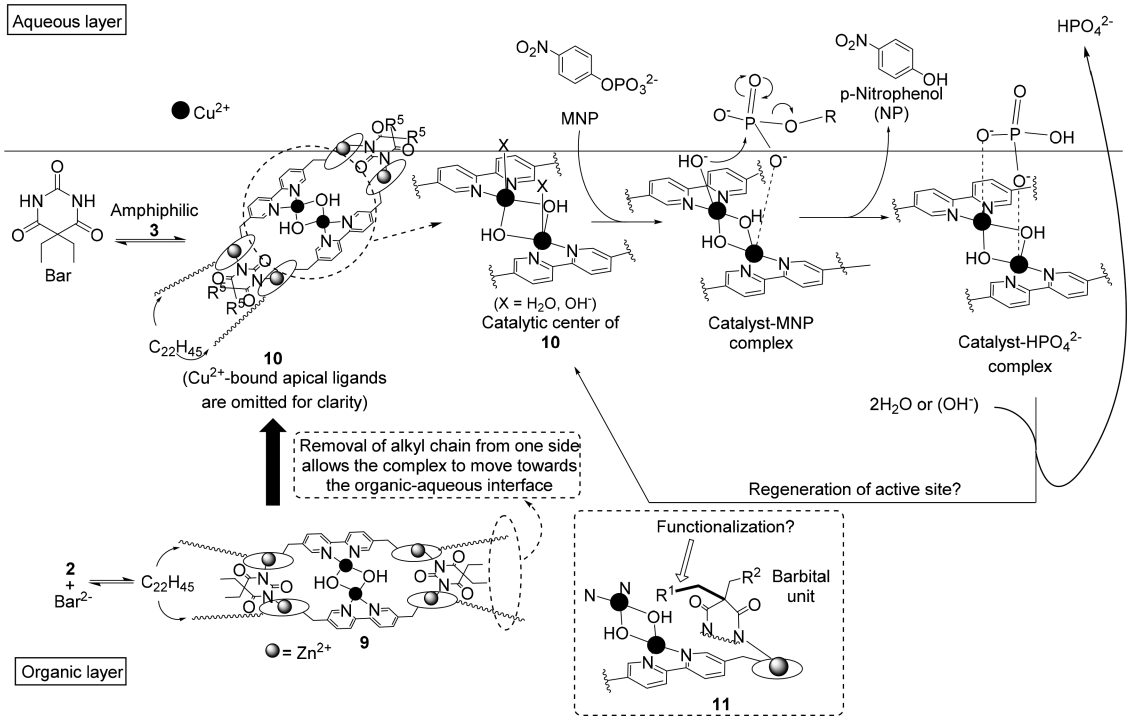

DOI: 10.1021/acs.inorgchem.8b03586
Inorg. Chem. XXXX, XXX, XXX−XXX

product and an inhibitor of the overall reaction (product inhibition).[2,11]

It is generally accepted that natural enzymes such as AP trap (extract) the specific substrates from aqueous phase around the enzymes into their hydrophobic catalytic pockets, accelerate the specific and selective reactions (e.g., the hydrolysis of phosphates in AP), and eventually release the products to aqueous phase, so that their catalytic sites are regenerated to accept the next substrate. On the basis of the structure of the hydrophilic complex **8**, as determined by X-ray crystal structure analysis,[9] a hydrophobic complex **9** (Scheme 1 and Scheme 2) was designed for use in a two-phase solvent system ($CHCl_3/H_2O$) to mimic the reaction sites and catalytic mechanism of AP as mentioned above.[10] It was expected that a bis(Zn^{2+}-cyclen) complex with two long alkyl chains **2** (Zn_2L^2), **4a** and Cu^{2+} would form a 2:2:2 complex **9**, which would be more stable in organic solvents than in an aqueous solution. It was hypothesized that Cu^{2+}-bound OH^- attacks the phosphorus of MNP, which is achieved by the coordination to the another Cu^{2+}.[12] It was also expected that product inhibition by HPO_4^{2-} could be avoided, since the hydrophilic HPO_4^{2-} would be released into the aqueous layer as it was formed, thus permitting the $Cu_2(\mu\text{-OH})_2$ center to be regenerated like catalytic reactions by natural enzymes (Scheme 2). Namely, we attempted at mimicking the catalytic function of AP not only by the structures of supramolecular complexes but also by the selection of appropriate solvent systems. Very interestingly, the hydrolysis of MNP by **9** followed Michaelis–Menten kinetics even in the two-phase solvent system containing $CHCl_3$ and H_2O. However, negligible catalytic turnover was observed, possibly due to low efficiency in the extraction of MNP by hydrophobic complex **9** toward the organic phase and/or the slow release of HPO_4^{2-} into the aqueous phase.

To address the aforementioned problems, we designed and synthesized a series of new supramolecular complexes by the self-assembly of a nonsymmetric amphiphilic dinuclear Zn^{2+}–cyclen complex containing one long alkyl chain **3** (Zn_2L^3) with Bar^{2-} derivatives and Cu^{2+} as artificial phosphatases (**10** in Scheme 1) that function in two-phase solvent system ($CHCl_3/H_2O$), in this work. We expected that the active sites, $Cu_2(\mu\text{-OH})_2$, of **10** would be localized in closer proximity to the organic–water interface than **9**, and hence product inhibition by the inorganic phosphate would be reduced by its release into the aqueous layer (Scheme 2). Moreover, the side chains of the Bar units were functionalized, because one of the two ethyl groups of each Bar unit in **8** are located in close proximity to the $Cu_2(\mu\text{-OH})_2$ catalytic site (**11** in a dashed box of Scheme 2), as confirmed by an X-ray crystal structure analysis of **8**.

Herein, we report on the self-assembly of **3**, the functionalized Bar units, and Cu^{2+} to form **10** and the catalytic activity of **10** for the MNP hydrolysis in a two-phase solvent system. Mechanistic aspects of its catalytic activity are discussed based on the UV/vis and emission spectra of the supramolecular complexes in H_2O and $CHCl_3$ layers of the reaction mixtures.

■ EXPERIMENTAL PROCEDURES

General Information. All reagents and solvents were of the highest commercial quality and were used without further purification, unless otherwise noted. Anhydrous dimethylformamide (DMF) was obtained by distillation from calcium hydride. Anhydrous CCl_4 was obtained by distillation. The Good's buffer reagents (Dojindo, pK_a at 20 °C) were obtained from commercial sources: HEPES, pK_a = 7.6. Stock aqueous solutions of 20 mM MNP were prepared using deionized and distilled water and stored at 0 °C prior to use. UV spectra were recorded on a JASCO V-550 spectrophotometer, equipped with a temperature controller unit operating at 25 ± 0.1 and 37 ± 0.1 °C. IR spectra were recorded on a Perkin–Elmer ATR-IR spectrum 100 at room temperature. Melting points were measured by a Yanaco MP-J3Micro Melting Point apparatus without any correction. ^{1}H (300 MHz) and ^{13}C (75 MHz) NMR spectra at 25 ± 0.1 °C were recorded on a JEOL Always 300 spectrometer. Tetramethylsilane (TMS) was used as internal reference for ^{1}H and ^{13}C NMR measurements by $CDCl_3$, deuterated dimethyl sulfoxide (DMSO-d_6) or CD_3OD. Mass spectra were recorded on a JEOL JMS-SX102A and Varian 910-MS. Elemental analyses were performed on a PerkinElmer CHN 2400 series II CHNS/O analyzer at the Research Institute for Science and Technology, Tokyo University of Science. Thin-layer chromatographies (TLC) and silica gel column chromatographies were performed using Merck Silica gel 60 F254 TLC plate or Fuji Silysia Chemical CHROMATOREX NH-TLC PLATE, and Fuji Silysia Chemical FL-100D or Fuji Silysia Chemical CHROMATOREX NH Chromatography Silica Gel, respectively.

Synthesis of 1-Docosyl-4,10-bis(tert-butyloxycarbonyl)-1,4,7,10-tetraazacyclododecane (16). A mixture of 1-bromodocosane **14** (0.63 g, 1.62 mmol) and sodium iodide (0.24 g, 1.62 mmol) in acetone (6.5 mL) and hexane (6.5 mL) was heated at reflux for 12 h under an argon atmosphere. On the completion of reaction, the insoluble compounds were removed by filtration and washed with hexane (10 mL). The filtrate was concentrated under reduced pressure to give **15** (0.71 g) as a colorless solid, which was used in the next step without further purification. To a solution of 1,7-bis(*tert*-butyloxycarbonyl)-1,4,7,10-tetraazacyclododecane **13** (0.55 g, 1.5 mmol) and potassium carbonate (0.2 g, 1.5 mmol) in MeCN (14 mL) and $CHCl_3$ (6 mL), **15** (0.71 g) in $CHCl_3$ (10 mL) was slowly added over a period of 15 min. The reaction mixture was stirred at room temperature for 3 d under argon atmosphere. After insoluble inorganic salts were removed by filtration, the filtrate was evaporated under reduced pressure. The remaining residue was purified by NH silica gel column chromatography ($CHCl_3$/MeOH = 100/1) to give **16** as a colorless oil (0.30 g, 29% yield). IR (attenuated total reflectance (ATR)) cm^{-1}: 3225, 2923, 2853, 1694, 1459, 1407, 1365, 1246, 1160, 861, 754. ^{1}H NMR (300 MHz, $CDCl_3$/TMS) δ: 3.40–3.25 (m, 8H), 2.85–2.62 (m, 8H), 2.53–2.47 (m, 2H), 1.45 (s, 18H), 1.25 (m, 40H), 0.88 (t, 3H, J = 6.6 Hz). ^{13}C NMR (75 MHz, $CDCl_3$/TMS) δ: 156.1, 155.8, 79.6, 79.4, 54.3, 53.7, 52.9, 50.3, 50.1, 49.8, 49.5, 49.2, 48.6, 48.4, 47.7, 47.4, 31.9, 29.8, 29.6, 29.6, 29.3, 28.4, 22.6, 14.1. Fast atom bombardment mass spectrometry (FAB-MS) m/z: 681.6256 (Calcd for $C_{40}H_{81}N_4O_4$ [M + H]$^+$: 681.6258).

Tris(tert-butyl)-10-((5′-(bromomethyl)-[2,2′-bipyridin]-5-yl)-methyl)-1,4,7,10-tetraazacyclododecane-1,4,7-tricarboxylate (19). A mixture of **12**[13] (0.46 g, 0.98 mmol), 5,5′-bis(bromomethyl)-2,2′-bipyridine **18** (0.40 g, 1.23 mmol), and sodium carbonate (0.59 g, 5.3 mmol) in MeCN (50 mL) was refluxed for 12 h under an argon atmosphere. After the reaction was completed, the mixture was evaporated and suspended in $CHCl_3$ (30 mL). The organic layer was washed with H_2O (20 mL × 3) and brine, dried over Na_2SO_4, and filtered, and the filtrate was evaporated under reduced pressure. The resulting residue was purified by silica gel column chromatography (hexane/AcOEt = 1/1) to give **19** as a pale brown oil (0.19 g, 25% yield). IR (ATR) cm^{-1}: 2975, 1683, 1596, 1552, 1463, 1414, 1364, 1248, 1153, 979, 752. ^{1}H NMR (300 MHz, $CDCl_3$/TMS) δ: 8.68 (d, 1H, J = 3 Hz), 8.54 (d, 1H, J = 0.9 Hz), 8.37 (t, 2H, J = 8.4 Hz), 7.85 (dd, 1H, J = 9 Hz, 2.1 Hz), 7.76 (dd, 1H, J = 6 Hz, 2.4 Hz, 2.1 Hz), 4.54 (s, 2H), 3.83 (s, 2H), 3.60–3.35 (m, 12H), 2.69 (brs, 4H), 1.48 (m, 27H). ^{13}C NMR (75 MHz, $CDCl_3$/TMS) δ: 155.8, 154.6, 137.5, 133.5, 120.9, 120.7, 79.6, 79.4, 55.4, 53.9, 50.0, 47.7, 29.6, 28.6, 28.4. FAB-MS m/z: 733.3281 (Calcd for $C_{35}H_{54}BrN_6O_6$ [M + H]$^+$: 733.3283).

1,4,7-Tris(tert-butoxycarbonyl)-10-((5′-((4,10-bis(tert-butoxycarbonyl)-7-docosyl-1,4,7,10-tetraazacyclododecan-1-yl)methyl)-[2,2′-bipyridin]-5-yl)methyl)-1,4,7,10-tetraazacyclododecane (20).

DOI: 10.1021/acs.inorgchem.8b03586
Inorg. Chem. XXXX, XXX, XXX–XXX

A mixture of **19** (0.20 g, 0.27 mmol), **16** (0.26 g, 0.38 mmol), and sodium carbonate (0.17 g, 1.6 mmol) in MeCN (10 mL) and $CHCl_3$ (10 mL) was heated at reflux temperature for 16 h under an argon atmosphere. After the reaction mixture was evaporated, the resulting residue was suspended in $CHCl_3$ (50 mL) and was then washed with H_2O (20 mL × 3) and brine, dried over Na_2SO_4, filtered, and evaporated under reduced pressure. The resulting residue was purified by silica gel column chromatography ($CHCl_3$/MeOH = 80/1) to give **20** as a yellow amorphous/solid (0.15 g, 28% yield). IR (ATR) cm^{-1}: 2923, 2853, 1687, 1595, 1551, 1458, 1411, 1364, 1247, 1152, 858, 751. ^1H NMR (300 MHz, $CDCl_3$/TMS) δ: 8.53 (d, 2H, J = 6.3 Hz), 8.31 (d, 2H, J = 7.5 Hz), 7.80 (d, 1H, J = 7.2 Hz), 7.74 (dd, 1H, J = 9.0 Hz, J = 1.5 Hz,), 3.83 (s, 2H), 3.71 (s, 2H), 3.61 (s, 4H), 3.39 (m, 14H), 2.65 (m, 12H), 2.41 (t, 2H, J = 7.2 Hz), 1.48−1.43 (m, 45H), 1.26 (s, 42H), 0.88 (t, 3H, J = 6.6 Hz). ^{13}C NMR (75 MHz, $CDCl_3$/TMS) δ: 155.8, 155.4, 150.5, 138.6, 135.3, 120.6, 120.5, 56.0, 55.5, 53.9, 50.0, 47.8, 45.6, 31.9, 29.7, 29.4, 28.7, 28.5, 27.8, 22.7, 14.1. ESI-MS m/z: 1334.0204 (Calcd. for $C_{75}H_{133}N_{10}O_{10}$ [M + H]$^+$: 1334.0201).

1-((5′-((1,4,7,10-Tetraazacyclododecan-1-yl)methyl)-[2,2′-bipyridin]-5-yl)methyl)-7-docosyl-1,4,7,10-tetraazacyclododecane·9HBr·2H$_2$O (21). To a solution of **20** (0.1 g, 75 μmol) in MeOH (3 mL) and $CHCl_3$ (3 mL), 47% HBr (2 mL) was slowly added at 0 °C. The resulting mixture was stirred at room temperature for 24 h and then concentrated under reduced pressure. The resulting residue was recrystallized from 47% HBr and MeOH to give **21** as a brown solid (0.1 g, 89% yield). IR (ATR) cm^{-1}: 3385, 2929, 2850, 2608, 1599, 1570, 1547, 1436, 1067, 931, 754, 722. ^1H NMR (300 MHz, DMSO-d_6/TMS) δ: 8.73 (s, 2H), 8.46 (d, 2H, J = 8.1 Hz), 8.10 (t, 2H, J = 11.1 Hz), 3.89 (d, 4H, J = 7.8 Hz), 3.22−3.13 (m, 16H), 2.88−2.77 (m, 16H), 1.46 (brs, 2H), 1.23 (s, 40H), 0.85 (t, 3H, J = 6.3 Hz). ^{13}C NMR data could not be obtained because of the low solubility of this material. Electrospray ionization mass spectrometry (ESI-MS) m/z: 833.7571 (Calcd for $C_{50}H_{93}N_{10}$ [M + H]$^+$: 833.7579). Anal. Calcd. for $C_{50}H_{105}Br_9N_{10}O_2$: C, 37.59; H, 6.62; N, 8.77. Found: C, 37.36; H, 6.46; N, 8.42%.

3·4ClO$_4$·2H$_2$O. The pH of an aqueous mixture (5 mL) of **21** as the HBr salt (60 mg) was adjusted to 12 with a 2 N NaOH aqueous solution, and the resulting solution was extracted with $CHCl_3$ (20 mL × 5). The combined organic layer was washed with brine, dried over Na_2SO_4, filtered, and concentrated under reduced pressure. The resulting deprotonated **21** (39 mg, 46 μmol) was dissolved in a mixture of MeOH (4 mL) and $CHCl_3$ (3 mL), to which a solution of $Zn(ClO_4)_2·6H_2O$ (35 mg, 92 μmol) in H_2O was added. The solution was stirred at 70 °C for 36 h. After the solvent was evaporated, the residue was crystallized from EtOH to give **3** as a pink solid (61 mg, 94% yield). mp >200 °C. IR (ATR) cm^{-1}: 3529, 3285, 2922, 2852, 1480, 1067, 958, 928, 853, 748, 720, 620. ^1H NMR (300 MHz, DMSO-d_6/TMS) δ: 8.70 (s, 2H), 8.44 (d, 2H, J = 8.1 Hz), 8.00 (d, 2H, J = 7.8 Hz), 4.76−4.49 (m, 4H), 3.95 (s, 4H), 2.95−2.89 (m, 4H), 2.78−2.68 (m, 24H), 1.53 (brs, 2H), 1.23 (s, 40H), 0.85 (t, 3H, J = 6.3 Hz) ppm. ^{13}C NMR data could not be obtained because of the low solubility of this material. FAB-MS m/z: 579.4 (Calcd for $C_{50}H_{92}Cl_2N_{10}O_8$ [M-2ClO$_4$]$^{2+}$: 579.2525). Anal. Calcd. for $C_{50}H_{96}Cl_4N_{10}O_{18}Zn_2$: C, 42.96; H, 6.92; N, 10.02. Found: C, 42.81; H, 6.74; N, 9.75%.

Diethyl 2,2-bis((benzyloxy)methyl)malonate (23). To a slurry of NaH (55 mg, 2.3 mmol, 55 wt % dispersion in oil) in distilled DMF (6 mL), diethyl melonate (**22**) in DMF (6 mL) was added, and the resulting solution was stirred for 30 min at 0 °C. Then ((chloromethoxy)methyl)benzene dissolved in distilled DMF (0.3 g, 1.92 mmol, purity >90%) was slowly added dropwise to the suspension. The resulting mixture was refluxed overnight under an argon atmosphere. After it cooled to room temperature, the mixture was neutralized with water and extracted with Et_2O. The organic layer was then washed with brine and dried over Na_2SO_4 and concentrated under reduced pressure. Residue was purified by silica gel chromatography (hexane/AcOEt = 30/1) to afford **23** as colorless oil (0.12 g, 37%). IR (ATR) cm^{-1}: 3463, 2859, 1730, 1454, 1301, 1204, 1075, 751, 692, 482. ^1H NMR (300 MHz, $CDCl_3$/TMS) δ: 7.33−7.23 (m, 10H), 4.51 (s, 4H), 4.17 (q, 4H, J = 6.9 Hz), 4.01 (s, 4H), 1.20 (t, 4H, J = 7.2 Hz). ^{13}C NMR (75 MHz, $CDCl_3$/TMS) δ: 168.2, 138.1, 127.4, 127.3, 73.2, 68.0, 61.3, 59.4, 13.9. FAB-MS m/z: 401.1963 (Calcd. for $C_{23}H_{28}O_6$ [M + H]$^+$: 401.1959).

5,5-Bis(benzyloxymethyl)barbituric acid (4b). Diethyl 2,2-bis-((benzyloxy)methyl)malonate **23** (0.11 g, 0.27 mmol) in freshly distilled DMF (1.5 mL) was added dropwise to a slurry of NaH (27 mg, 1.1 mmol, 55 wt % dispersion in oil) and urea (0.12 g, 1.9 mmol) in freshly distilled DMF (3 mL) at 0 °C. The mixture was stirred at 100 °C for 24 h. After it cooled to room temperature, water was added to the mixture, which was then extracted with Et_2O. The combined organic layers were washed with brine and dried over Na_2SO_4. The solvents were evaporated, and the resulting oil was purified by silica gel chromatography ($CHCl_3$) to afford **4b** as a colorless solid (16 mg, 16%). mp 165−168 °C. IR (ATR) cm^{-1}: 3417, 3222, 1751, 1696, 1425, 1341, 1228, 1089, 835, 732, 614, 493. ^1H NMR (300 MHz, $CDCl_3$/TMS) δ: 7.34−7.16 (m, 10H), 4.45 (s, 4H), 3.76 (s, 4H). ^{13}C NMR (75 MHz, $CDCl_3$/TMS) δ: 170.5, 148.6, 136.7, 128.5, 128.0, 127.5, 73.7, 71.1, 58.8. FAB-MS m/z: 369.1447 (Calcd. for $C_{23}H_{28}O_6$ [M + H]$^+$: 369.1445). Anal. Calcd. for $C_{23}H_{28}O_6$: C, 65.21; H, 5.47; N, 7.60. Found: C, 65.19; H, 5.29; N, 7.39%.

Hydrolysis of MNP. The hydrolysis reaction of MNP was performed in $CHCl_3$/50 mM HEPES buffer (pH 7.4 with I = 0.1 ($NaNO_3$)) (2/8) (total volume 3.0 mL) in the presence of **10a−f** (final concentration: 20 μM in the total solution), and all the hydrolysis reactions were triplicated. Stock solutions of barbital derivatives (**4a−f**) (6.0 mM in $CHCl_3$), $Cu(ClO_4)_2·6H_2O$ (6.0 mM in H_2O), HEPES (100 mM in H_2O, pH 7.4 with I = 0.2 ($NaNO_3$)), and MNP (20 mM in H_2O) were prepared, respectively. Prior to the MNP hydrolysis, the reaction mixtures of **4a−f** (or **3**) and Cu^{2+} in $CHCl_3$/50 mM HEPES buffer (pH 7.4 with I = 0.1 ($NaNO_3$)) were incubated at 37 °C for 1 d using shaking water bath (shaking speed: 150 rpm) (PersonalH incubator) to form **10a−f** in situ. After this, a given volume (15 to ∼150 μL) of an aqueous solution of 20 mM MNP was added to start the hydrolysis of MNP, and all the hydrolysis experiments were performed at 37 °C using shaking water bath (shaking speed: 150 rpm). The aqueous and organic layers of the reaction mixtures were separated by centrifugation (3000 rpm × 10 min at 25 ± 0.1 °C) at a given time (from day 0 up to day 7), and the UV/vis absorption spectra of the aqueous layer were measured to determine the concentrations of 4-nitrophenol (4-NP) (the ε_{400} value of NP is 1.35 × 10^4 $M^{-1}·cm^{-1}$ at pH 7.4 in aqueous solution), a hydrolysis product from MNP, to calculate the yields of MNP hydrolysis ([NP produced in the presence of the supermolecule] − [4-NP produced in the absence of the supermolecule]). The partition ratio of 4-NP (79% in aqueous solution) was used for calculation of yields in $CHCl_3/H_2O$ system based on our previous paper.[10]

■ RESULTS AND DISCUSSION

Synthesis of a Dimeric Zn^{2+} Complex Containing One Long Alkyl Chain. A bis(Zn^{2+}−cyclen) containing a bpy unit and one long alkyl chain (in one cyclen unit) **3** (Zn_2L^3) was synthesized as shown in Scheme 3. Cyclen was reacted with di-*tert*-butyldicarbonate (Boc_2O) and *N*-(*tert*-butoxycarbonyl)-succinimide (Boc-OSu) to give 3-Boc-cyclen **12**[13] and 2-Boc-cyclen **13**,[14] respectively, according to the previously reported procedures. The monoalkylation of **13** with 1-iododocosane **15**, prepared from 1-bromodocosane **14**, afforded **16**. The alkylation of 5,5′-bis(bromomethyl)-2,2′-bipyridine **18**[8,15,16] obtained from 5,5′-dimethyl-2,2′-bipyridine **17** with **12** in the presence of Na_2CO_3 gave **19**. After **19** reacted with **16** to produce **20**, the Boc protecting groups were removed by the treatment with aqueous HBr, giving **21** as a HBr salt. The acid-free **21** was obtained by extracting with $CHCl_3$ from 2 N NaOH and then reacted with 2 equiv of $Zn(ClO_4)_2·6H_2O$ to afford **3** (Zn_2L^3).

DOI: 10.1021/acs.inorgchem.8b03586
Inorg. Chem. XXXX, XXX, XXX−XXX

Scheme 3. Synthesis of 3 (Zn_2L^3)

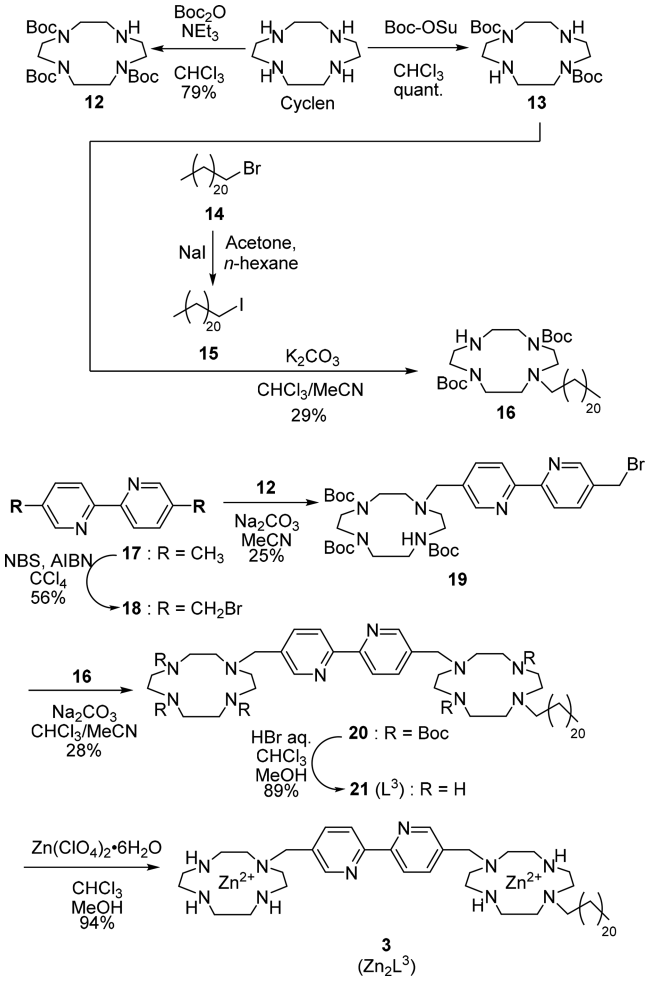

Scheme 4. Structures of the 2:2:2 Complexes 10a–f Formed from 7a–f (2:2 Complexes of 3 and 4a–f) and Cu^{2+}

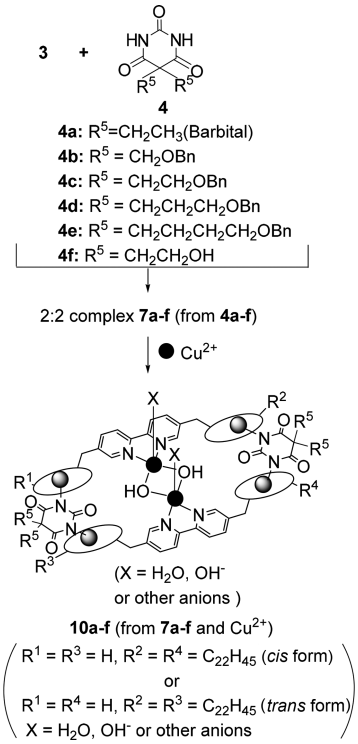

Complexation Behavior of 3 with Bar^{2-} and Cu^{2+} As Studied by UV/Vis Titrations. Because **3** was not soluble in either organic or aqueous solutions, UV/vis titrations of **3** with barbital (Bar^{2-}) and its derivatives **4a–4f** and $Cu(ClO_4)_2 \cdot 6H_2O$ were performed in dimethyl sulfoxide (DMSO)/50 mM HEPES buffer (pH 7.4, with I = 0.1 ($NaNO_3$) (4/96) at 37 °C (Scheme 4). The slight increase in the absorption of **3** (20 μM) at 287 nm was observed upon the addition of Bar^{2-}, reaching a plateau at a 1:1 ratio, as shown in the inset of Figure S2 in Supporting Information, suggesting that 2:2 complexation of **3** with Bar^{2-} had occurred.

UV/Vis titrations of **7a** (10 μM) with Cu^{2+} in DMSO/50 mM HEPES buffer (pH 7.4 with I = 0.1 ($NaNO_3$) (4/96)) were conducted at 37 °C. Figure S3 in Supporting Information shows a red shift in the absorption maxima of **7a** from ca. 287 to ca. 307 nm reaching a plateau at [Cu^{2+}]/[**7a**] = 2.0 (the inset of Figure S3 in Supporting Information), indicating that 1:2 complexation of **7a** and Cu^{2+} had occurred. It was also indicative of the quantitative formation of **10a** at the micromolar order.

UV/Vis titrations of **3** (Zn_2L^3 itself) (40 μM) with Cu^{2+} in DMSO/50 mM HEPES buffer (pH 7.4 with I = 0.1 ($NaNO_3$) (4/96)) were also performed at 37 °C for the comparison with the UV/vis titrations of **7a** with Cu^{2+} described above. As shown in Figure S4 in Supporting Information, the UV/vis spectra exhibited a red-shift from ca. 287 to ca. 308 nm, which reached a plateau at [Cu^{2+}]/[**3**] = 1.0 (the inset of Figure S4 in Supporting Information), indicating that the 1:1 complexation of **3** and Cu^{2+}, which is different from the 1:2 complexation of **7a** and Cu^{2+}.

Hydrolysis of MNP by 2:2:2 Complexes in Two-Phase Solvent Systems. The hydrolysis of MNP (100 μM) was performed in $CHCl_3$/50 mM HEPES buffer (pH 7.4 with I = 0.1 ($NaNO_3$)) (2/8) in the presence of **10a** (prepared from **3**, Bar^{2-} **4a** and Cu^{2+}, [**10a**] = 20 μM in the total solution including organic and aqueous layers) at 37 °C. As shown in Figure S5 in Supporting Information (UV/vis spectral change of the aqueous layers of the reaction mixtures during the MNP hydrolysis producing 4-NP, which has strong absorbance at 400 nm) and Figure 1a, **10a** (20 μM in the total solution) accelerated the hydrolysis of MNP, and its initial rate was higher than the analogous reaction promoted by **9** (20 μM) in the same solvent system. Interestingly, we also found that the hydrolysis by **10a** proceeded in ca. 35% yield. Negligible acceleration was observed in the presence of **3** alone, Bar^{2-} alone, and Cu^{2+} alone under the same conditions. The hydrolysis of MNP by the **3** + Cu^{2+} complex was also accelerated, albeit in a noncatalytic manner. Figure 1b displays that the MNP hydrolysis by **10a** at [MNP] = 100, 200, 500, and 1000 μM and [**10a**] = 20 μM (namely, at [**10a**]/[MNP] = 20%, 10%, 4% and 2%) affords more than 20 μM of 4-NP (indicated with a dashed line in Figure 1b), suggesting that **10a** functions as a catalyst for the hydrolysis of MNP.

In the proposed structure of **10c** (formed from **3**, **4c**, and Cu^{2+}) generated by Mercury, Ver: 3.10 software based on the crystal structure of **8** (Figure 2a, in which Cu^{2+}-bound H_2O molecules are omitted for clarity), it was assumed that the benzyl groups of **4b–e** units in **10b–e** are located close to the $Cu_2(\mu\text{-}OH)_2$ sites and provide a hydrophobic environment for the substrate as shown in Figure 2b (the C_{22} alkyl groups are oriented to the same direction (a so-called *cis* conformer) in

DOI: 10.1021/acs.inorgchem.8b03586
Inorg. Chem. XXXX, XXX, XXX–XXX

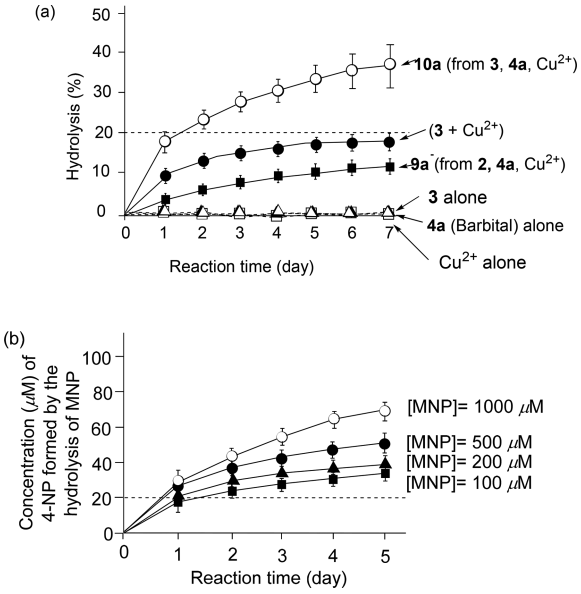

Figure 1. (a) Hydrolysis (%) of MNP (100 μM in the total solution) by **10a** (20 μM) (○), **3** + Cu^{2+} (40 μM) (●), **9a** (20 μM) (■), **3** (40 μM) (△), **4a** (40 μM) (▲), and Cu^{2+} only (40 μM) (□) in $CHCl_3$/50 mM HEPES buffer (pH 7.4 with I = 0.1 ($NaNO_3$)) (2/8) at 37 °C. (b) Concentrations of 4-NP, which is produced by the MNP hydrolysis, at [MNP] = 100 μM (■), 200 μM (▲), 500 μM (●), and 1000 μM (○), promoted by **10a** (20 μM) in $CHCl_3$/50 mM HEPES buffer (pH 7.4 with I = 0.1 ($NaNO_3$)) (2/8) at 37 °C. The initial concentrations of MNP and supramolecular complexes were determined in the total solution of the two-phase solvent systems. A dashed line in Figure 1b indicates that the concentration of **10a** is 20 μM.

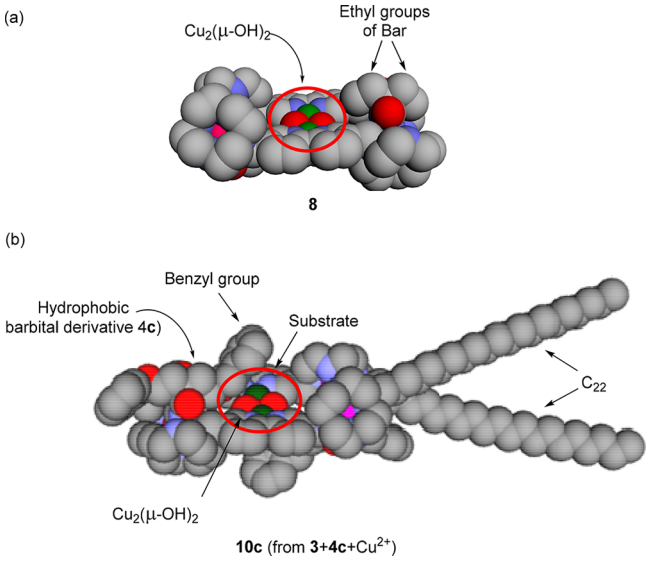

Figure 2. (a) X-ray crystal structure of **8**[9] and (b) proposed structure of the amphiphilic supermolecule **10c** (assuming a *cis* form, in which two alkyl groups are hypothesized to be orientated to the same side).

this structure, and there must also be *trans* form, as indicated in Scheme 4).

This assumption allowed us to synthesize the functionalized barbital derivatives **4b**−**f** that are shown in Scheme 5. The 2,2′-disubstituted malonates **23**−**26** were prepared by the dialkylation of diethyl malonate **22**, and successive cyclization with urea afforded the corresponding barbital derivatives **4b**−**f**,

Scheme 5. Synthesis of Functionalized Barbital Derivatives 4b−f

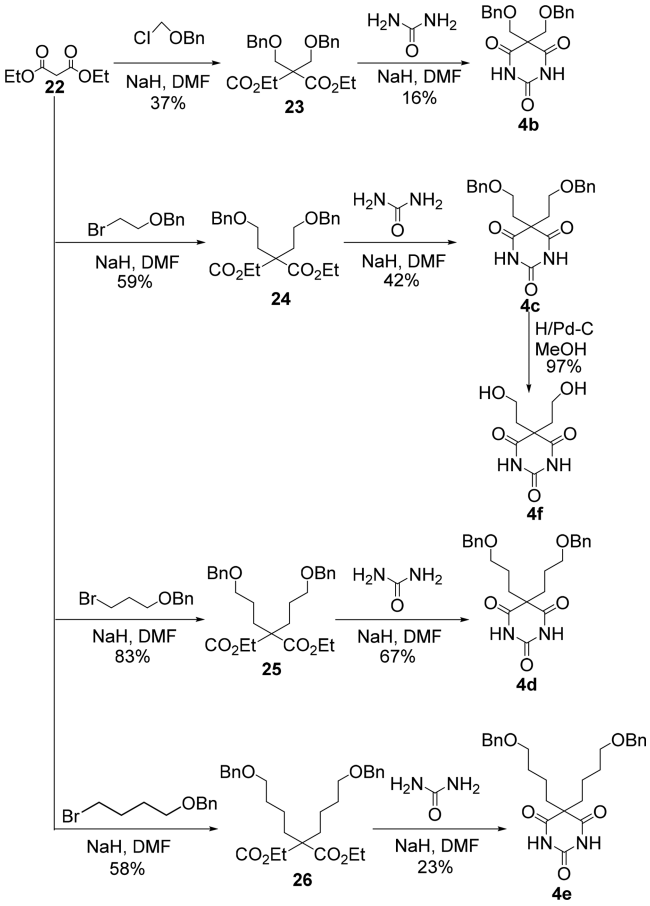

respectively (only **4b** was newly synthesized in this work).[9,13] Deprotection of the benzyl groups[17] of **4c** afforded **4f** having hydroxylethyl groups.

Hydrolysis of MNP by 2:2:2 Complexes Formed Reacting 3 (Zn_2L^3) with Barbital Derivatives and Cu^{2+} and Their Phosphate Hydrolysis Activity in Two-Phase Solvent Systems. Supramolecular complexes **10a**−**f** were prepared in situ from **3** (Zn_2L^3), Bar derivatives **4a**−**f**, and Cu^{2+}, and their MNP hydrolysis activity was then evaluated in $CHCl_3$/50 mM HEPES buffer (pH 7.4 with I = 0.1 ($NaNO_3$)) (2/8) at [MNP] = 100 μM and [**10a**−**f**] = 20 μM (in total solution) at 37 °C. As shown in Figure 3a, it was found that **10b**−**f** hydrolyzed MNP in over 20% yield, similar to **10a**. The hydrolysis of MNP by **10a**−**f** was also performed at [MNP] = 1000 μM and [**10**] = 20 μM (2% equivalent to MNP) (Figure 3b). As summarized in Figure 4, catalytic turnover numbers (CTN) for **10a**−**f** were determined to be higher than 3, while our previous supramolecular complexes **8** and **9** negligibly functioned as catalysts.

Michaelis−Menten Kinetics for Hydrolysis of MNP by 10a−f in Two-Phase Solvent Systems. The kinetics of the hydrolysis of MNP by **9** and **10a**−**f** was studied by the reaction at [MNP] = 100, 200, 500, 800, and 1000 μM (in total $CHCl_3/H_2O$ solvent) for 24 h at 37 °C. In a Lineweaver−Burk plot (Figure S6 in Supporting Information), the concentrations of MNP and the produced NP in the total solution of the two-phase solvent systems were used for the calculation (V_0 = initial hydrolysis rate), from which the approximate V_{max} (the

DOI: 10.1021/acs.inorgchem.8b03586
Inorg. Chem. XXXX, XXX, XXX−XXX

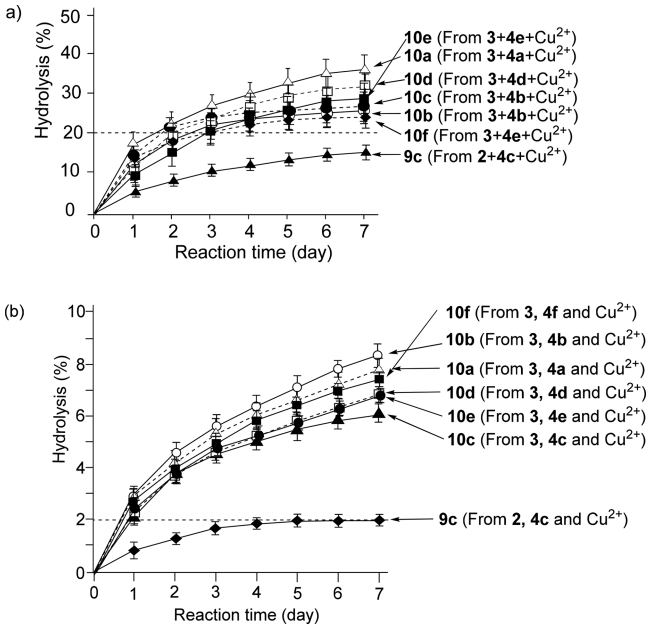

Figure 3. Time course for the hydrolysis (%) of MNP at [MNP] = 100 μM (a) and [MNP] = 1000 μM (b) by **9** and **10a–f** (20 μM in total solution) in $CHCl_3$/50 mM HEPES buffer (pH 7.4 with I = 0.1 ($NaNO_3$)) (2/8) at 37 °C. The initial concentrations of MNP and supramolecular complexes were determined in the total solution of the two-phase solvent system.

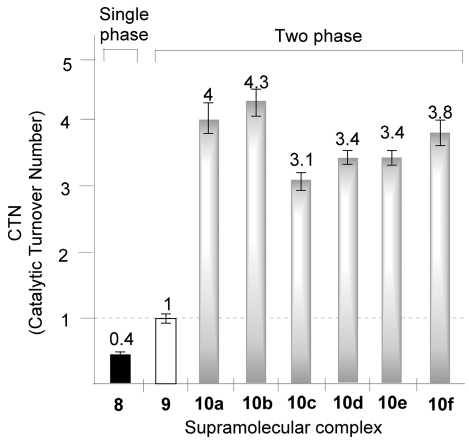

Figure 4. Comparison of CTN of **8**, **9**, and **10a–f** at [MNP] = 1000 μM and [**8**, **9**, or **10**] = 20 μM (in the total solution) in $CHCl_3$/50 mM HEPES buffer (pH 7.4 with I = 0.1 ($NaNO_3$)) (2/8) at 37 °C.

maximum rate in the NP production from MNP) of **10a–f** was calculated to be $(6.8 \pm 0.3) \times 10^{-2}$, $(3.4 \pm 0.3) \times 10^{-2}$, $(5.9 \pm 0.2) \times 10^{-2}$, $(2.0 \pm 0.3) \times 10^{-1}$, $(2.8 \pm 0.2) \times 10^{-2}$, and $(2.8 \pm 0.1) \times 10^{-2}$ μM/min, respectively, as summarized in Table 1. The K_m (Michaelis constant) values for **10a–f** were determined to be $(3.8 \pm 0.2) \times 10^2$, $(4.4 \pm 0.3) \times 10^2$, $(1.4 \pm 0.3) \times 10^2$, $(1.6 \pm 0.1) \times 10^3$, $(1.7 \pm 0.3) \times 10^2$, and $(1.2 \pm 0.2) \times 10^2$ μM, respectively. Their k_{cat} values defined by eq 1 are also listed in Table 1.

$$k_{cat} = V_{max}/K_m \quad (1)$$

The K_m values in Table 1 are compared with the K_d values of Cu^{2+} complexes **27** (CuL^4) reported by Esteban-Gómez et al.[18a,b] and **28** (CuL^5) synthesized by Delgado et al.[18c] with phosphates (Scheme 6). For instance, the complexation constant (log K_s) of **27** (CuL^4) with inorganic phosphate ($H_2PO_4^-$) in DMSO was reported to be 5.1, from which the K_d value was calculated to be ca. 80 μM.[18a] The log K_s value of **28** (CuL^5) with $H_2PO_4^-$ in a 1:1 mixture of MeOH/H_2O was reported to be 4.1, meaning that the K_d value for the Cu_2L^5–$H_2PO_4^-$ is 87 μM.[18c] We consider that K_m values of **10a–f** determined in a two-phase solvent system ($CHCl_3$/H_2O), as listed in the Table 1, are almost compatible to the K_d values of **27** and **28** with $H_2PO_4^-$ determined in organic solution or a mixture of MeOH/H_2O (single phase).

Scheme 6. Structures of Cu^{2+} Complexes Reported by Esteban-Gómez et al.[18a] and Delgado et al.[18c]

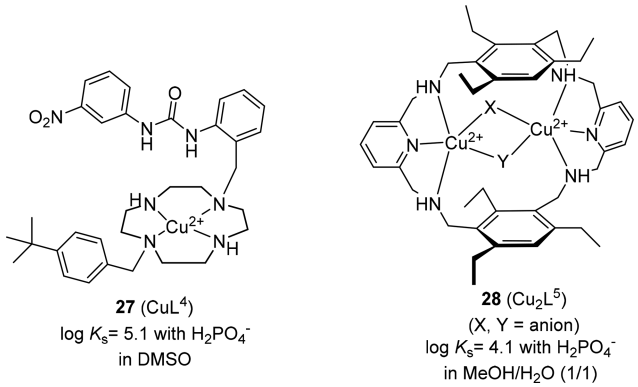

It is known that HPO_4^{2-}, a hydrolysis product of MNP, inhibits AP (product inhibition).[2,11] In Figure 3a,b, it was indicated that **10**-catalyzed MNP hydrolysis rate becomes slower as the reaction proceeds, possibly because of the

Table 1. Kinetic Parameters (V_{max}, K_m, k_{cat} and K_i of Inorganic Phosphate) for Hydrolysis of MNP by 8, 9, 10a–f and AP

	V_{max} (1 μM·min^{-1})	K_m (μM)	k_{cat} (min^{-1})	K_i (μM)	K_m/K_i
8[a]	$(8.9 \pm 0.2) \times 10^{-2}$ [b]	$(4.1 \pm 0.3) \times 10^2$ [b]	$(2.2 \pm 0.2) \times 10^{-4}$ [b]	ca. 15 (mixed-type)[b]	ca. 27
9[c]	$(1.4 \pm 0.4) \times 10^{-2}$ [c]	$(5.4 \pm 0.5) \times 10^2$ [c]	$(2.7 \pm 0.4) \times 10^{-5}$	ca. 15 (competitive)	ca. 36
10a[d]	$(6.8 \pm 0.3) \times 10^{-2}$	$(3.8 \pm 0.2) \times 10^2$	$(1.8 \pm 0.2) \times 10^{-4}$	ca. 80 (mixed-type)	ca. 4.8
10b[d]	$(3.4 \pm 0.3) \times 10^{-2}$	$(4.4 \pm 0.3) \times 10^2$	$(7.8 \pm 1) \times 10^{-5}$	ca. 98 (mixed-type)	ca. 4.5
10c[d]	$(5.9 \pm 0.2) \times 10^{-2}$	$(1.4 \pm 0.3) \times 10^2$	$(4.5 \pm 0.9) \times 10^{-4}$	nd[e]	nd[e]
10d[d]	$(2.0 \pm 0.3) \times 10^{-1}$	$(1.6 \pm 0.1) \times 10^3$	$(1.3 \pm 0.2) \times 10^{-4}$	nd[e]	nd[e]
10e[d]	$(2.8 \pm 0.2) \times 10^{-2}$	$(1.7 \pm 0.3) \times 10^2$	$(1.7 \pm 0.4) \times 10^{-4}$	nd[e]	nd[e]
10f[d]	$(2.8 \pm 0.1) \times 10^{-2}$	$(1.2 \pm 0.2) \times 10^2$	$(2.5 \pm 0.5) \times 10^{-4}$	nd[e]	nd[e]
AP[f]	1.3 ± 0.1[f]	7 ± 4[f]	$(2.4 \pm 0.2) \times 10^3$ [f]	3 ± 1 (competitive)[f]	ca. 2.3

[a]From ref 9 (in a single aqueous phase). [b]Determined in a single aqueous solution (10 mM HEPES buffer, pH 7.4). [c]From ref 10. [d]Data of **10a–f** were obtained in $CHCl_3$/50 mM HEPES buffer (pH 7.4) (2/8). [e]Not determined. [f]From ref 5g.

DOI: 10.1021/acs.inorgchem.8b03586
Inorg. Chem. XXXX, XXX, XXX–XXX

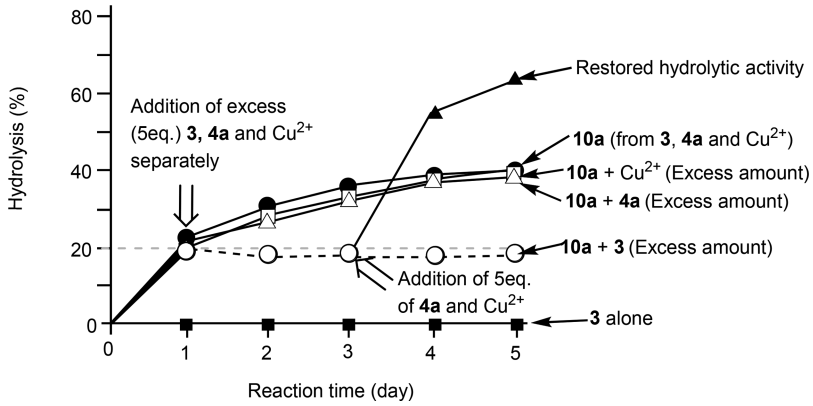

Figure 5. Hydrolysis of MNP at [MNP] = 100 μM in total solution by **10a** (●) (20 μM) as control, **10a** with excess (5 equiv) of **3** (200 μM) from day 1 (dashed curve with ○) and 5 equiv of (**4a** + Cu^{2+}) (200 μM) in the same vial from day 3 (▲), **3** alone (■) (40 μM), **10a** with excess (5 equiv) of **4a** (△) (200 μM), **10a** with excess (5 equiv) of Cu^{2+} (□) (200 μM) in $CHCl_3$/50 mM HEPES buffer (pH 7.4) with I = 0.1 ($NaNO_3$) (2/8) at 37 °C.

Scheme 7. Our Hypothesis for the Inhibition of MNP Hydrolysis by 10a upon the Addition of an Excess Amount of 3

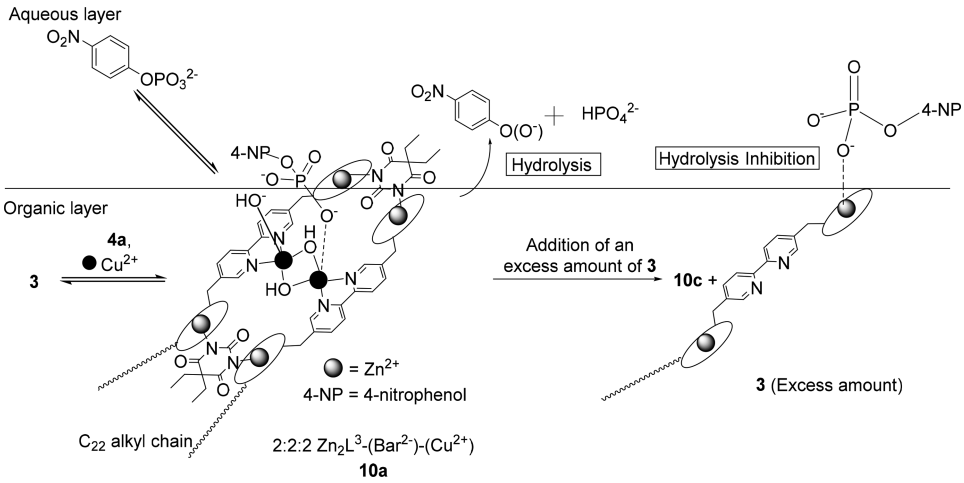

product inhibition. Therefore, MNP hydrolysis by **10a** and **10b** in the presence of HPO_4^{2-} was performed (at the initial [HPO_4^{2-}] = 0, 10, and 50 μM). The Lineweaver–Burk plot in Figure S7 in Supporting Information suggests that [HPO_4^{2-}] exhibits mixed-type inhibition,[19] and its K_i values against **10a** and **10b** were estimated to be ca. 80 and ca. 98 μM, respectively (Table 1).[20] The complex **10f** showed the smallest K_m value, which was ca. 3.4–4.5 times smaller than those of **8** and **9**, respectively. On the other hand, the K_i values of HPO_4^{2-} against **10a** and **10b** are ca. 5–6 times higher than those against **8** and **9**, and the K_m/K_i ratios of **10a** and **10b** are 4.5–4.8, which are much smaller than those of **8** and **9** (27–36) and are almost comparable to that of AP (2.3). These kinetic data suggest that **10a–f** have lower affinity to HPO_4^{2-} than that of **9**, possibly due to their closer localization to the aqueous–organic interface, resulting in more efficient release of HPO_4^{2-}, as we expected in Scheme 2.

Inhibitory Effect of 3 (Zn_2L^3) on the MNP Hydrolysis. As mentioned above (Figure 1a), the activity of **3** (Zn_2L^3) itself in the MNP hydrolysis was negligible. During our experiments, we found that the addition of a slight excess of Zn_2L^3 against Bar^{2-} (**4a**) unit and Cu^{2+} resulted in a decrease in the MNP hydrolysis rates. Therefore, we suspected that the presence of Zn_2L^3 had an inhibitory effect on the hydrolysis of MNP, although it is normally predicted that Zn^{2+} complexes would accelerate the hydrolysis of phosphate esters and other ester substrates. As shown in Figure 5, the addition of an excess amount of **3** 1 d after starting the hydrolysis of MNP (100 μM) by **10a** (20 μM) caused a considerable inhibition in the hydrolysis (dashed curve with open circles). To overcome this inhibitory effect, an excess amount of **4a** and Cu^{2+} was added on day 3 in the same vial, and this addition restarted the MNP hydrolysis (plain curve with closed triangles). We conclude that **3** likely binds to MNP at the $CHCl_3/H_2O$ interface, resulting in the inhibition of MNP hydrolysis by **10a**, as presented in Scheme 7. The addition of excess amount of **4a**(open triangles) or Cu^{2+} (open squares) to **10a** had no effect on the hydrolysis of MNP, as shown in Figure 5.

Hydrolysis of Bis(4-nitrophenyl)phosphate (BNP) by 2:2:2 Complexes in Two-Phase Solvent Systems. The hydrolysis of BNP (200 μM, 500 μM, 800 μM, and 1 mM) was also performed in $CHCl_3$/50 mM HEPES buffer (pH 7.4 with I = 0.1 ($NaNO_3$)) (2/8) in the presence of **10a** (prepared from **3**, Bar^{2-} **4a**, and Cu^{2+}) ([**10a**] = 20 μM in the total solution including organic and aqueous layers) at 37 °C (Figure 6). In this case, the hydrolysis reaction proceeded in ca. 24% yield catalyzed by **10a** (when [BNP] = 1 mM and [**10a**] = 20 μM (indicated with a dashed line in Figure 6) and, hence, [**10a**]/[BNP] = 0.02), indicating that it catalyzes hydrolysis of BNP (CTN is up to ca. 12), as well.

DOI: 10.1021/acs.inorgchem.8b03586
Inorg. Chem. XXXX, XXX, XXX–XXX

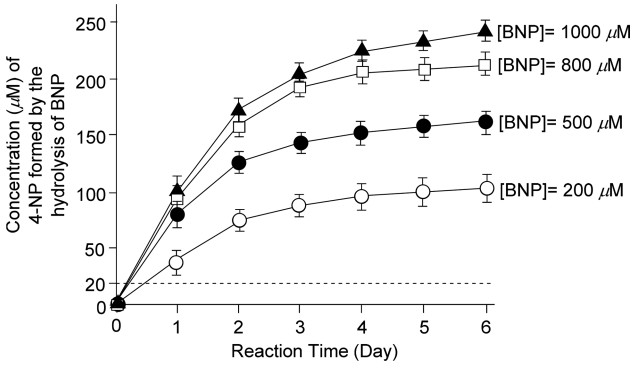

Figure 6. Hydrolysis of BNP at [BNP] = 1000 μM (▲), 800 μM (□), 500 μM (●), and 200 μM (○) by **10a** (20 μM) in $CHCl_3$/50 mM HEPES buffer (pH 7.4 with I = 0.1 ($NaNO_3$)) (2/8) at 37 °C. A dashed line indicates the concentration of **10a**.

Location of Complexes 8, 9, and 10a in the Two-Phase Solvent System, As Determined from UV/Vis and Emission Spectra of H_2O and $CHCl_3$ Phases. To elucidate how and why **10a**−**f** function as catalysts for the hydrolysis of MNP and BNP, the location of the supramolecular complexes in the two-phase solvent system was examined. Namely, Zn_2L alone (**1**, **2**, **3**), 2:2 complex of Zn_2L and Bar^{2-} (**5**, **6**, **7a**), and 2:2:2 complex of Zn_2L, Bar^{2-}, and Cu^{2+} (**8**, **9**, **10a**) were prepared in $CHCl_3$/50 mM HEPES (pH 7.4, I = 0.1 ($NaNO_3$)) (1/1), shaken vigorously, and then centrifuged (2000 rpm × 10 min) at room temperature.

Figure 7a,b shows the pictures of Zn_2L (**1**, **2**, and **3**) (100 μM) under sunlight and under irradiation at 365 nm, respectively. Although the difference between a control sample that contains no Zn^{2+} complex (Ctrl) and **1** under sunlight (Figure 7a) was negligible, a strong emission in $CHCl_3$ layer was observed for **2** and at the interface of $CHCl_3/H_2O$ layers

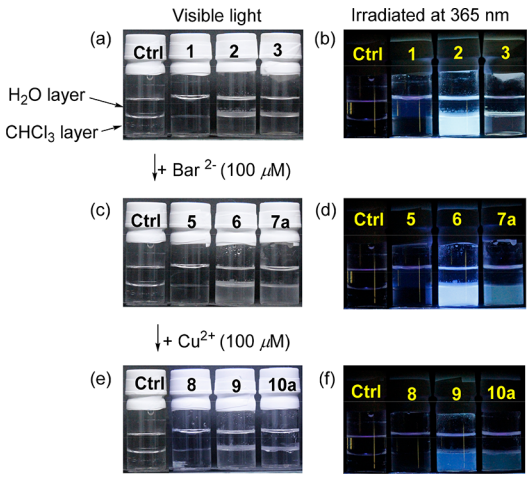

Figure 7. Pictures of mixtures of Zn_2L and their complexes with Bar and Cu^{2+} in $CHCl_3$/50 mM HEPES (pH 7.4 with I = 0.1 ($NaNO_3$)) (50/50)). Upper layer is the aqueous layer, and the lower one is $CHCl_3$. Each sample was incubated for 12 h at 37 °C with rigorous stirring and centrifuged (2000 rpm × 10 min). (a, b) Vials of control that include only solvents (Ctrl), **1**, **2**, and **3** (100 μM) from left under sunlight (a) and irradiation at 365 nm (b). (c, d) Vials of control containing only solvents (Ctrl), **5**, **6**, and **7a** (50 μM) from left under sunlight (c) and irradiation (d) at 365 nm. (e, f) Vials of control (Ctrl), **8**, **9**, and **10a** (50 μM) from left under sunlight (e) and irradiation at 365 nm (f).

for **3** (Figure 7b), indicating that **1** remains in the aqueous layer, **2** (soluble in $CHCl_3$) is distributed mainly in the $CHCl_3$ layer, and **3** (insoluble in both water and $CHCl_3$) is located mainly at the aqueous−organic interface. Similarly, the data shown in Figure 7c,d suggest that **5** and **6** are present in the same location as were **1** and **2** and that small amounts of **3** moved to the $CHCl_3$ layer by complexation with Bar^{2-} (by the formation of **7a**). The addition of 100 μM of Cu^{2+} to the solutions of **5**, **6**, and **7a** resulted in the emission in all the layers being reduced, as shown in Figure 7f, possibly because the emission of the bpy unit in supramolecular complexes is quenched by Cu^{2+}.

For a more detailed analysis, UV/vis absorption and emission spectra of the aqueous and organic layers were measured after these two layers were separated by centrifugation. As shown in Figure 8a, UV/vis absorption spectra of aqueous layers for Zn_2L (**1**, **2**, and **3**) exhibit absorption maxima in the 280−320 nm region, and the concentration of **1** (Zn_2L^1) was found to be much higher than those (dashed curve) of **2** (Zn_2L^2) (blue curve) and **3** (red curve). On the contrary, the concentration of **2** was highest in $CHCl_3$ layer, and the concentration of **3** (Zn_2L^3, depicted in a red bold line) was between those of **1** and **2** (Figure 8b). Similar behavior was observed for the 2:2 complexes, **5**, **6**, and **7a** (Figure 8c,d). The addition of Cu^{2+} to solutions of **5**, **6**, and **7a** exhibited similar result in the UV/vis spectra of both aqueous and organic layers, as shown in Figure 8e,f, respectively.

For comparison, UV/vis absorption and emission spectra of nonfunctionalized bpy were obtained in both aqueous and $CHCl_3$ solutions.[21] Since bpy is not soluble in H_2O, a stock solution of bpy in DMSO was prepared and diluted with H_2O or $CHCl_3$, respectively, for the measurement. From the UV/vis spectral curves of bpy in the H_2O and $CHCl_3$ layers (Figure S8a,b in Supporting Information), the absorption coefficients (ε) of bpy in H_2O and $CHCl_3$ layers were calculated to be ca. 6.9×10^3 and ca. 7.7×10^3 M^{-1} cm^{-1}, respectively. Since **1**−**3** and **5**−**7a** contain two bpy units, we estimated the distribution (%) (Table 2) of each complex (**5**, **6**, and **7a**) in each phase using equations derived from the Beer−Lambert law (eqs 2 and 3 in Scheme S2 in Supporting Information). As summarized in Table 2, the finding indicates that more than 98% of **5** remains in the H_2O layer and that most (>99%) of **6** is located in the $CHCl_3$ layer. In contrast, **7a** is distributed in both the H_2O layer (ca. 35%) and the $CHCl_3$ layer (ca. 65%).

Figure 9 shows the emission spectra of **1**−**3** and **5**−**7** in the H_2O and $CHCl_3$ layers (emission spectra of **8**−**10a** that include Cu^{2+} are not shown, because these emissions are quenched by Cu^{2+}). Note that **6** has emission maxima at ca. 330 and ca. 480 nm in the $CHCl_3$ layer (a blue curve) and that **7a** has broad emission curve from 320 to 550 nm (a red curve) in Figure 9d. For comparison, Figure S8c,d in Supporting Information shows fluorescent emission maxima of bpy in H_2O and $CHCl_3$ layers at 330 and 370 nm, respectively, not around 500 nm, indicating that emission of **7a** at ∼500 nm is due to the complexation of **3** with barbital (**4a**).

It was previously reported that the emission of bpy in silica gel glass is at ca. 400 and ca. 450 nm.[22] It was also reported that the emission of bpy is at ca. 400 and ca. 450 nm in EtOH at high concentration (0.1 M), while only one emission maxima was observed at ca. 400 nm at a concentration of 3 mM. Such a dual emission of bpy at ca. 400 and ca. 450 nm

DOI: 10.1021/acs.inorgchem.8b03586
Inorg. Chem. XXXX, XXX, XXX−XXX

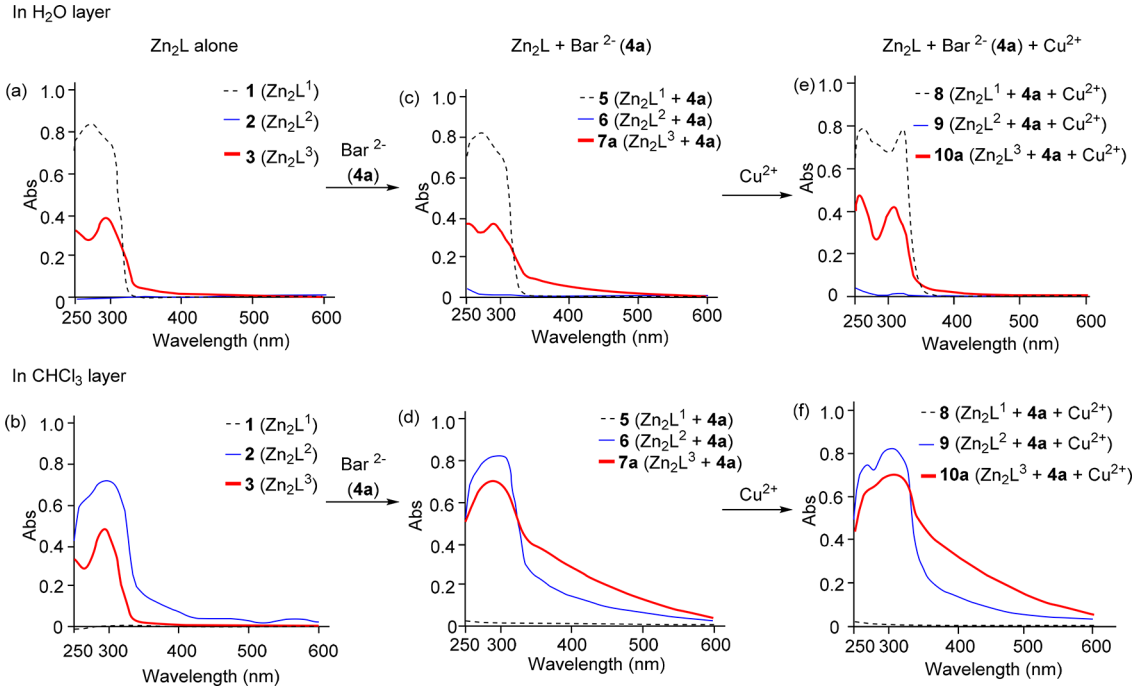

Figure 8. UV/Vis absorption spectra of aqueous and $CHCl_3$ layers separated from the two-phase solvent system including Zn_2L, **4a**, and Cu^{2+} ($[Zn_2L] = [Bar^{2-}$ (**4a**)$] = [Cu^{2+}] = 100$ μM in the initial two-phase solvent system) at 37 °C. (a, b) UV/Vis absorption spectra of **1**, **2**, and **3** in H_2O layer (a) and $CHCl_3$ layer (b). (c, d) UV/Vis spectra of **5**, **6**, and **7a** in H_2O layer (c) and $CHCl_3$ layer (d). (e, f) UV/Vis absorption spectra of **8**, **9**, and **10a** in H_2O layer (e) and $CHCl_3$ layer (f).

Table 2. Approximate Distribution (%) of 5, 6, and 7a in the H_2O Layer and the $CHCl_3$ Layer after Separation of Two-Phase Solvent Systems [5, 6, 7a] = 50 μM in a Mixture of $CHCl_3/H_2O$ Estimated by UV/Vis Spectra of These Complexes in H_2O and $CHCl_3$, As Shown in Figure 8

Complex	in H_2O layer (%)	in $CHC1_3$ layer (%)
5	>98%	<2%
6	<1%	>99%
7a	ca. 35%	ca. 65%

can be explained by the excimer formation among several bpy molecules in silica gel and in EtOH at high concentrations.

In our work, hydrophilic **1** (100 μM) exhibited an emission maximum at ca. 390 nm with a small shoulder at ca. 340 nm, and **5** (50 μM formed from 100 μM **1** and 100 μM **4a**) exhibits mainly two emission maxima at ca. 380 and at ca. 500 nm in a single aqueous phase, as shown in Figure S9 in Supporting Information.[23] As described in the Introduction, 2:2 complexes of Zn_2L and Bar^{2-} (**5**, **6**, and **7a**) include two bpy units that are arranged in a parallel manner due to the $\pi-\pi$ stacking interaction, which possibly induce an excimer emission at ca. 500 nm, as shown in Figure 9c,d. These facts support the formation and distribution of **7a** in H_2O and $CHCl_3$ layers, as shown in Figure 7d and 9c,d. It is also suggested that **2** and **3** themselves are present in the form of aggregates in $CHCl_3$ layers, which exhibit excimer emission (Figure 9b).

These facts allow us to conclude that the supramolecular catalyst **10** is located in both the aqueous layer and organic layer in these systems, and its hydrophobicity/hydrophilicity balance is a key factor for the catalytic hydrolysis of MNP. The efficient extraction of MNP from the aqueous layer to the organic layer and the successful release of inorganic phosphate

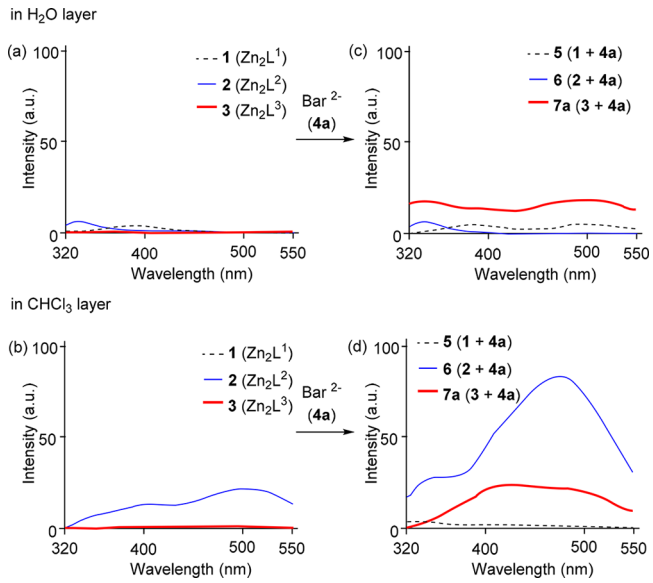

Figure 9. (a, b) Emission spectra of **1**, **2**, and **3** in aqueous layer (a) and in $CHCl_3$ layer (b) (correspond to samples of Figure 8a,b, respectively) at 25 °C. (c, d) Emission spectra of **5**, **6**, and **7a** in aqueous layer (c) and $CHCl_3$ layer (d) at 25 °C (correspond to samples of Figure 8c,d, respectively) (excitation at 293 nm) (a.u. is arbitrary unit).

from the organic layer to the aqueous layer also appear to be important factors.

■ CONCLUSION

In conclusion, we report on the formation of supramolecular complexes **10** by the 2:2:2 self-assembly of **3**, functionalized Bar^{2-} units (**4a–f**), and Cu^{2+} as well as their catalytic activity

DOI: 10.1021/acs.inorgchem.8b03586
Inorg. Chem. XXXX, XXX, XXX−XXX

for the hydrolysis of a phosphate monoester, MNP. The findings indicate that the hydrolysis of MNP by **10a−f** (20 μM in the total solution, 0.2−0.02 equiv vs MNP) in a two-phase solvent system proceeds catalytically. Moreover, the hydrolysis of MNP by these supramolecular complexes obeys Michaelis−Menten kinetics in two-phase solvent systems, and the calculated K_m values for **10a−f** are smaller as well as K_i of HPO_4^{2-} values are higher than those for **8** and **9**. In addition, the overall CTNs of **10a−f** are ∼3−4, and their K_m/K_i values (4.5−4.8) are close to that of AP (2.3) and much smaller than those of noncatalytic supramolecular complexes **8** and **9** (27−36). To the best of our knowledge, this is the first example of the formation of artificial catalysts by the self-assembly of three components (**3**, Bar^{2-} blocks (**4a−f**) and Cu^{2+}) (or four components, i.e., Zn^{2+}, **21** (L^3), **4a−f**, and Cu^{2+}) for the catalytic hydrolysis of a phosphate monoester, MNP, in two-phase solvent system. This work along with our previous works and mechanistic studies based on the distribution of supramolecular complexes suggest that the hydrophilicity/hydrophobicity balance of the complexes is important for the catalytic hydrolysis of phosphate monoester. The results reported here should be useful in the future design of stable, biologically active, and biocompatible supramolecular complexes.

It is well-established that catalytic reactions using phase transfer catalysts in two-phase solvent systems (liquid−liquid, liquid−solid, etc.) are powerful methods for organic synthesis, especially for asymmetric synthesis using chiral phase-transfer catalysts.[24] However, kinetic aspects and detailed mechanisms of these reactions are yet to be studied. The information described in this manuscript might be important in terms of understanding the mechanism of the catalytic activity of natural enzymes such as AP and that of artificial catalysts including chiral phase-transfer catalysts.

One of other remaining questions in this work is the stereochemistry of **10a−f**. In this work, we considered that **10a−f** can exist in both a *cis* form, in which their two C_{22} alkyl side chains are oriented in the same direction, and in a *trans* form, in which the two C_{22} alkyl groups are oriented in the opposite directions, in the reaction mixtures (Scheme 1, Scheme 4, and Figure 2b). The design and synthesis of new Zn^{2+} complexes that can be used to answer this question as well as the design and synthesis of Bar^{2-} units equipped with functional groups for achieving higher NMP hydrolysis activity are currently underway.

■ ASSOCIATED CONTENT

Supporting Information

The Supporting Information is available free of charge on the ACS Publications website at DOI: 10.1021/acs.inorgchem.8b03586.

Possible mechanism of MNP hydrolysis, pH rate profile, UV/vis titration data, UV/vis spectra, Liveweaver−Burke plots, estimated distributions of **5**, **6**, **7a**, **8**, **9**, and **10a** (PDF)

■ AUTHOR INFORMATION

Corresponding Author

*E-mail: shinaoki@rs.noda.tus.ac.jp. Phone: +81-4-7121-3670.

ORCID

Shin Aoki: 0000-0002-4287-6487

Notes

The authors declare no competing financial interest.

■ ACKNOWLEDGMENTS

This work was supported by grants-in-aid from the Ministry of Education, Culture, Sports, Science and Technology (MEXT) of Japan (No. 17K0826 for Y.S. and Nos. 24640156, 15K00408, 16K10396, and 17K08225 for S.A.) and "Academic Frontiers" project for private universities: matching funds from MEXT, and the Tokyo University of Science (TUS) fund for strategic research areas. We wish to acknowledge Ms. T. Matsuo (Research Institute for Science and Technology, TUS) for the elemental analysis. We appreciate the aid of Mrs. F. Hasegawa (Faculty of Pharmaceutical Sciences, TUS) and Mrs. N. Sawabe (Faculty of Pharmaceutical Sciences, TUS) for measurement of mass spectra and ^{1}H NMR spectra.

■ REFERENCES

(1) (a) Millan, J. L. Alkaline Phosphatases Structure, substrate speciliacity and functional relatedness to other members of a large superfamily of enzymes. *Purinergic Signalling* **2006**, *2*, 335−341. (b) O'Brie, P. J.; Herschlag, D. Functional Interrelationships in the Alkaline Phosphatase Superfamily: Phosphodiesterase Activity of Escherichia coli Alkaline Phosphatase. *Biochemistry* **2001**, *40*, 5691−5699. (c) Woodgett, J. *Protein Kinase Functions, Frontiers in Molecular Biology;* Oxford University Press: Oxford, U.K., **2000**. (d) Denu, J. M.; Stuckey, J. A.; Saper, M. A.; Dixon, J. E. Form and Function in Protein Dephosphorylation. *Cell* **1996**, *87*, 361−364. (e) Hegg, E. L.; Burstyn, J. N. Toward the development of metal-based synthetic nucleases and peptidases: a rationale and progress report in applying the principles of coordination chemistry. *Coord. Chem. Rev.* **1998**, *173*, 133−165. (f) Kramer, R. *Coord. Chem. Rev.* **1999**, *182*, 243−261.

(2) (a) Averill, B. A. *In comprehensive Coordination Chemistry II;* Que, L., Jr., Tolman, W. B., Eds.; Elsevier: Amsterdam, The Netherlands, 2003; Vol. *8*, pp 641−676. (b) Christianson, D. W.; Cox, J. D. Catalysis by Metal-Activated Hydroxide in Zinc and Manganese Metalloenzymes. *Annu. Rev. Biochem.* **1999**, *68*, 33−57. (c) Vallee, B. L.; Auld, D. S. Zinc: Biological Functions and Coordination Motifs. *Acc. Chem. Res.* **1993**, *26*, 543−551. (d) Auld, D. S. Zinc Coordination Sphere in Biochemical Zinc Sites. *BioMetals* **2001**, *14*, 271−313. (e) Cleland, W. W.; Hengge, A. C. Enzymatic Mechanisms of Phosphate and Sulfate Transfer. *Chem. Rev.* **2006**, *106*, 3252−3278. (f) Kimura, E. DimetallicHydrolases and their Models. *Curr. Opin. Chem. Biol.* **2000**, *4*, 207−213. (g) Aoki, S.; Kimura, E. In Bio-coordination Chemistry. Zinc Hydrolases*Comprehensive Coordination Chemistry II;* Que, L., Jr., Tolman, W. B., Eds.; Elsevier: Amsterdam, The Netherlands, 2003; Vol. *8*, pp 601−640. (h) Weston, J. Mode of Action of Bi- and Trinuclear Zinc Hydrolases and Their Synthetic Analogues. *Chem. Rev.* **2005**, *105*, 2151−2174. (i) Cotton, F. A.; Wilkinson, G. *Advances in Inorganic Chemistry: A Comprehensive Text,* 5th ed.; Wiley-VCH: New York, 1988; Vol. *1*. (j) Holtz, K. M.; Kantrowitz, E. R. *FEBS Lett.* **1999**, *462*, 7−11. (k) Wilson, I. B.; Dayan, J.; Katherine, C. Some Properties of Alkaline Phosphatase from Escherichia coli : TRANSPHOSPHORYLATION. *J. Biol. Chem.* **1964**, *239*, 4182−4185. (l) Kim, E. E.; Wyckoff, H. W. Reaction mechanism of alkaline phosphatase based on crystal structures. *J. Mol. Biol.* **1991**, *218*, 449−464.

(3) For reviews, see: (a) Vahrenkamp, H. Transitions, Transition States, Transition State Analogues: Zinc Pyrazolylborate Chemistry Related to Zinc Enzymes. *Acc. Chem. Res.* **1999**, *32*, 589−596. (b) Suh, J. Synthetic Artificial Peptidases and Nucleases Using Macromolecular Catalytic Systems. *Acc. Chem. Res.* **2003**, *36*, 562−570. (c) Garcia-Espana, E.; Diaz, P.; Llinares, J. M.; Bianchi, A. Anion Coordination Chemistry in Aqueous Solution of PolyammoniumReceptors. *Coord. Chem. Rev.* **2006**, *250*, 2952−2986. (d) Natale, D.; Mareque-Rivas, J. C. The Combination of Transition Metal Ions and Hydrogen-bonding Interactions. *Chem. Commun.* **2008**, 425−437.

DOI: 10.1021/acs.inorgchem.8b03586
Inorg. Chem. XXXX, XXX, XXX−XXX

(e) Mewis, R. E.; Archibald, S. J. Biomedical Applications of Macrocyclic Ligand Complexes. *Coord. Chem. Rev.* **2010**, *254*, 1686−1712. (f) Mitic, N.; Smith, S. J.; Neves, A.; Guddat, L. W.; Gahan, L. R.; Schenk, G. The Catalytic Mechanisms of Binuclear Metallohydrolases. *Chem. Rev.* **2006**, *106*, 3338−3363.

(4) For reference about hydrolysis of phosphate diesters, see: (a) Kaminskaia, N. V.; He, C.; Lippard, S. J. Reactivity of μ-Hydroxodizinc(II) Centers in Enzymatic Catalysis through Model Studies. *Inorg. Chem.* **2000**, *39*, 3365−3373. (b) Jeung, C.-S.; Song, J. B.; Kim, Y.-H.; Suh, J. Hydrolysis of Linear DNA Duplex Catalyzed by Co(III) Complex of Cyclen Attached to Polystyrene. *Bioorg. Med. Chem. Lett.* **2001**, *11*, 3061−3064. (c) Ait-Haddou, H.; Sumaoka, J.; Wiskur, S. L.; Folmer-Andersen, J. F.; Anslyn, E. V. Remarkable Cooperativity between a Zn^{II} Ion and Guanidinium/Ammonium Groups in the Hydrolysis of RNA. *Angew. Chem., Int. Ed.* **2002**, *41*, 4013−4016. (d) Scarso, A.; Scheffer, U.; Göbel, M.; Broxterman, Q. B.; Kaptein, B.; Formaggio, F.; Toniolo, C.; Scrimin, P. A Peptide Template as an Allosteric Supramolecular Catalyst for the Cleavage of Phosphate Esters. *Proc. Natl. Acad. Sci. U. S. A.* **2002**, *99*, 5144−5149. (e) Humphry, T.; Forconi, M.; Williams, N. H.; Hengge, A. C. Altered Mechanisms of Reactions of Phosphate Esters Bridging a Dinuclear Metal Center. *J. Am. Chem. Soc.* **2004**, *126*, 11864−11869. (f) Andrew Knight, D.; Delehanty, J. B.; Goldman, E. R.; Bongard, J.; Streich, F.; Edwards, L. W.; Chang, E. L. Carboxylic Acid Functionalized Cobalt(III) CyclenComplexes for Catalytic Hydrolysis of Phosphodiester Bonds. *Dalton Trans.* **2004**, 2006−2011. (g) Jikido, R.; Shiraishi, H.; Matsufuji, K.; Ohba, M.; Furutachi, H.; Suzuki, M.; Okawa, H. Mass Spectrometric and Spectroscopic Studies on Hydrolysis of Phosphoesters by BisphenolatoDinuclearMetal(II) Complexes (Metal = Mn, Co, Ni, and Zn). *Bull. Chem. Soc. Jpn.* **2005**, *78*, 1795−1803. (h) Maldonado Calvo, J. A.; Vahrenkamp, H. A New *Tris* (2-furyl) Substituted PyrazolylborateLigand and its Zinc Complex Chemistry. *Inorg. Chim. Acta* **2005**, *358*, 4019−4026. (i) Mardolado Calvo, J. A.; Vahrencamp, H. A New *Tris* (2-furyl) Substituted PyrazolylborateLigand and its Zinc Complex Chemistry. *Inorg. Chim. Acta* **2006**, *359*, 4079−4086. (j) Jiang, F.; Huang, L.; Meng, X.; Du, J.; Yu, X.; Zhao, Y.; Zeng, X. MetallomicellarCatalysis: Hydrolysis of Phosphate Monoester and Phosphodiester by Cu(II), Zn(II) Complexes of Pyridyl ligands in CTAB Micellar Solution. *J. Colloid Interface Sci.* **2006**, *303*, 236−242. (k) Sumaoka, J.; Chen, W.; Kitamura, Y.; Tomita, T.; Yoshida, J.; Komiyama, M. Application of Cerium(IV)/EDTA Complex for Future Biotechnology. *J. Alloys Compd.* **2006**, *408−412*, 391−395. (l) Belousoff, M. J.; Duriska, M. B.; Graham, B.; Batten, S. R.; Moubaraki, B.; Murray, K. S.; Spiccia, L. Synthesis, X-ray Crystal Structures, Magnetism, and Phosphate Ester Cleavage Properties of Copper(II) Complexes of *N*-Substituted Derivatives of 1, 4,7-Triazacyclononane. *Inorg. Chem.* **2006**, *45*, 3746−3755. (m) Feng, G.; Mareque-Rivas, J. C.; Williams, N. H. Comparing a Mononuclear Zn(II) Complex with Hydrogen Bond Donors with a Dinuclear Zn(II) Complex for CatalysingPhosphate Ester Cleavage. *Chem. Commun.* **2006**, *303*, 1845−1847. (n) Feng, G.; Natale, D.; Prabaharan, R.; Mareque-Rivas, J. C.; Williams, N. H. Efficient Phosphodiester Binding and Cleavage by a Zn^{II} Complex Combining Hydrogen-Bonding Interactions and Double Lewis Acid Activation. *Angew. Chem., Int. Ed.* **2006**, *45*, 7056−7059. (o) Perez Olmo, C.; Bohmerle, K.; Vahrenkamp, H. Zinc Enzyme Modelling with Zinc Complexes of Polar PyrazolylborateLigands. *Inorg. Chim. Acta* **2007**, *360*, 1510−1516. (p) Mancin, F.; Tecilla, P. Zinc(II) Complexes as Hydrolytic Catalysts of Phosphate Diester Cleavage: From Model Substrates to Nucleic Acids. *New J. Chem.* **2007**, *31*, 800−817. (q) Cartuyvels, E.; Absillis, G.; Parac-Vogt, T. N. Questioning the Paradigm of Metal Complex Promoted Phosphodiester Hydrolysis: $[Mo_7O_{24}]^{6-}$Polyoxometalate Cluster as an Unlikely Catalyst for the Hydrolysis of a DNA Model Substrate. *Chem. Commun.* **2008**, 85−87. (r) Takebayashi, S.; Shinkai, S.; Ikeda, M.; Takeuchi, M. Metal Ion Induced Allosteric Transition in the Catalytic Activity of an Artificial Phosphodiesterase. *Org. Biomol. Chem.* **2008**, *6*, 493−499. (s) Bonomi, R.; Selvestrel, F.; Lombardo, V.; Sissi, C.; Polizzi, S.; Mancin, F.; Tonellato, U.; Scrimin, P. Phosphate Diester and DNA Hydrolysis by a Multivalent, Nanoparticle-Based Catalyst. *J. Am. Chem. Soc.* **2008**, *130*, 15744−15756. (t) Taran, O.; Medrano, F.; Yatsimirsky, A. K. Rapid Hydrolysis of Model Phosphate Diesters by Alkaline-earth Cations in Aqueous DMSO: Speciation and Kinetics. *Dalton Trans.* **2008**, 6609−6618. (u) Subat, M.; Woinaroschy, K.; Gerstl, C.; Sarkar, B.; Kaim, W.; Konig, B. 1,4,7,10-Tetraazacyclododecane Metal Complexes as Potent Promoters of Phosphodiester Hydrolysis under Physiological Conditions. *Inorg. Chem.* **2008**, *47*, 4661−4668. (v) Penkova, L. V.; Maciag, A.; Rybak-Akimova, E. V.; Haukka, M.; Pavlenko, V. A.; Iskenderov, T. S.; Kozlowski, H.; Meyer, F.; Fritsky, I. O. Efficient Catalytic Phosphate Ester Cleavage by Binuclear Zinc(II) Pyrazolate Complexes as Functional Models of Metallophosphatases. *Inorg. Chem.* **2009**, *48*, 6960−6971. (w) Piovezan, C.; Jovito, R.; Bortoluzzi, A. J.; Terenzi, H.; Fischer, F. L.; Severino, P. C.; Pich, C. T.; Azzolini, G. G.; Peralta, R. A.; Rossi, L. M.; Neves, A. HeterodinuclearFe^{III}Zn^{II}-Bioinspired Complex Supported on 3-Aminopropyl Silica. Efficient Hydrolysis of Phosphate Diester Bonds. *Inorg. Chem.* **2010**, *49*, 2580−2582. (x) Bonomi, R.; Scrimin, P.; Mancin, F. Phosphate Diesters Cleavage Mediated by Ce(IV) Complexes Self-Assembled on Gold Nanoparticles. *Org. Biomol. Chem.* **2010**, *8*, 2622−2626. (y) Katz, M. J.; Mondloch, J. E.; Totten, R. K.; Park, J. K.; Nguyen, S. T.; Farha, O. K.; Hupp, J. T. Simple and Compelling Biomimetic Metal-Organic Framework Catalyst for the Degradation of Nerve Agent Simulants. *Angew. Chem., Int. Ed.* **2014**, *53*, 497−501. (z) Zhamoitina, A. I.; Sauerwein, Y.; König, B.; Arslanov, V. V.; Kalinina, M. A. A Binary Catalytic System Based on Mixed Monolayers of Phospholipid and Amphiphilic Bis(Zn^{2+}-cyclen). *Colloid J.* **2014**, *76*, 153−160. (aa) Tirel, E. Y.; Williams, N. H. Enhancing Phosphate Diester Clevage by Zinx Complex through Controlling Nucleophile Coordination. *Chem. - Eur. J.* **2015**, *21*, 7053−7056.

(5) For references of artificial compounds that accelerate the hydrolysis of phosphate monoesters, see: (a) Seo, J. S.; Sung, N.-D.; Hynes, R. C.; Chin, J. Structure and Reactivity of a DinuclearCobalt(III) Complex with a Bridging Phosphate Monoester. *Inorg. Chem.* **1996**, *35*, 7472−7473. (b) Williams, N. H.; Lebuis, A.-M.; Chin, J. A Structural and Functional Model of DinuclearMetallophosphatases. *J. Am. Chem. Soc.* **1999**, *121*, 3341−3348. (c) Williams, N. H.; Takasaki, B.; Wall, M.; Chin, J. Structure and Nuclease Activity of Simple Dinuclear Metal Complexes: Quantitative Dissection of the Role of Metal Ions. *Acc. Chem. Res.* **1999**, *32*, 485−493. (d) Vance, D. H.; Czarnik, A. W. Functional Group Convergency in a Binuclear Dephosphorylation Reagent. *J. Am. Chem. Soc.* **1993**, *115*, 12165−12166. (e) Koike, T.; Inoue, M.; Kimura, E.; Shiro, M. Novel Properties of Cooperative DinuclearZinc(II) Ions: The Selective Recognition of Phosphomonoesters and Their PO Ester Bond Cleavage by a New Dinuclear Zinc(II) Cryptate. *J. Am. Chem. Soc.* **1996**, *118*, 3091−3099. (f) Hettich, R.; Schneider, H.-J. Cobalt(III) Polyamine Complexes as Catalysts for the Hydrolysis of Phosphate Esters and of DNA. A Measurable 10 Million-Fold Rate Increase. *J. Am. Chem. Soc.* **1997**, *119*, 5638−5647. (g) Zulkefeli, M.; Suzuki, A.; Shiro, M.; Hisamatsu, Y.; Kimura, E.; Aoki, S. Selective Hydrolysis of Phosphate Monoester by Supramolecular Phosphatase Formed by the self-assembly of a Bis(Zn^{2+}-cyclen) Complex, Cyanuric Acid, and Copper in an Aqueous Solution (Cyclen = 1,4,7,10-Tetraazacyclododecane). *Inorg. Chem.* **2011**, *50*, 10113−10123. (h) Der, B. S.; et al. Catalysis by a De Novo Zinc-Mediated Protein Interface: Implications for Natural Enzyme Evolution and Rational Enzyme Engineering. *Biochemistry* **2012**, *51*, 3933−3940. (i) Zhang, X.; Zhu, Y.; Zheng, X.; Phillips, D. L.; Zhao, C. Mechanistic Investigation on the Cleavage of Phosphate Monoester Catalyzed by Unsymmetrical Macrocyclic Dinuclear Complexes: The Selection of Metal Centers and Intrinsic Flexibility of the Ligand. *Inorg. Chem.* **2014**, *53*, 3354−33361. (j) Xue, S.-S.; Zhao, M.; Ke, Z.-F.; Cheng, B.-C.; Su, H.; Cao, H.; Cao, K. C.; Wang, J.; Ji, L.-N.; Mao, Z.-W. Enantioselective Hydrolysis of Amino Acid Esters Promoted by Bis(β-cyclodextrin) Copper Complexes. *Sci. Rep.* **2016**, *6*, 22080.

(6) For review, see: (a) Conn, M. M.; Rebek, J., Jr. Self-Assembling Capsules. *Chem. Rev.* **1997**, *97*, 1647−1668. (b) Fujita, M. *Molecular*

DOI: 10.1021/acs.inorgchem.8b03586
Inorg. Chem. XXXX, XXX, XXX−XXX

Self-Assembly Organic Versus Inorganic Approaches Vol. *96*; Springer: Berlin, **2000**.177 (c) Breit, B. Supramolecular Approaches to Generate Libraries of Chelating Bidentate Ligands for Homogeneous Catalysis. *Angew. Chem., Int. Ed.* **2005**, *44*, 6816−6825. (d) Kleij, A. W.; Reek, J. N. H. Ligand-Template Directed Assembly: An Efficient Approach for the Supramolecular Encapsulation of Transition-Metal Catalysts. *Chem. - Eur. J.* **2006**, *12*, 4218−4227. (e) Oshovsky, G. V.; Reinhoudt, D. N.; Verboom, W. Supramolecular Chemistry in Water. *Angew. Chem., Int. Ed.* **2007**, *46*, 2366−2393. (f) Hannon, M. J. Supramolecular DNA Recognition. *Chem. Soc. Rev.* **2007**, *36*, 280−295. (g) van Leeuwen, P. W. N. M. *Supramolecular Catalysis;* Wiley-VCH: New York, 2008. (h) Koblenz, T. S.; Wassenaar, J.; Reek, J. N. H. Reactivity within a Confined Self-Assembled Nanospace. *Chem. Soc. Rev.* **2008**, *37*, 247−262. (i) Suzuki, K.; Tominaga, M.; Kawano, M.; Fujita, M. Self-assembly of an M_6L_{12}Coordination Cube. *Chem. Commun.* **2009**, 1638−1640. (j) Northrop, B. H.; Zheng, Y.-R.; Chi, K.-W.; Stang, P. J. Self-Organization in Coordination-Driven Self-Assembly. *Acc. Chem. Res.* **2009**, *42*, 1554−1563. (k) Leung, K. C.-F.; Chak, C.-P.; Lo, C.-M.; Wong, W.-Y.; Xuan, S.; Cheng, C. H.K. pH-Controllable Supramolecular Systems. *Chem. - Asian J.* **2009**, *4*, 364−381. (l) Yoshizawa, M.; Klosterman, J. K.; Fujita, M. Functional Molecular Flasks: New Properties and Reactions within Discrete, Self-Assembled Hosts. *Angew. Chem., Int. Ed.* **2009**, *48*, 3418−3438. (m) Yoshizawa, M.; Fujita, M. Development of Unique Chemical Phenomena within Nanometer-Sized, Self-Assembled Coordination Hosts. *Bull. Chem. Soc. Jpn.* **2010**, *83*, 609−618. (n) Trabolsi, A.; Khashab, N.; Fahrenbach, A. C.; Friedman, D. C.; Colvin, M. T.; Coti, K. K.; Benitez, D.; Tkatchouk, E.; Olsen, J.-C.; Belowich, M. E.; Carmielli, R.; Khatib, H. A.; Goddard, W. A., III; Wasielewski, M. R.; Stoddart, J. F. Radically Enhanced Molecular Recognition. *Nat. Chem.* **2010**, *2*, 42−49. (o) Meeuwissen, J.; Reek, J. N. H. Supramolecular Catalysis Beyond Enzyme Mimics. *Nat. Chem.* **2010**, *2*, 615−621. (p) Ma, Z.; Moulton, B. Recent Advances of Discrete Coordination Complexes and Coordination Polymers in Drug Delivery. *Coord. Chem. Rev.* **2011**, *255*, 1623−1641. (q) Aoki, S.; Zulkefeli, M.; Hisamatsu, Y.; Kitamura, M. Supramolecular Hosts and Catalysts Formed by Synergistic Molecular Assemblies of Multinuclear Zinc(II) Complexes in Aqueous Solution. In *Synergy in Supramolecular Chemistry;* Nabeshima, T., Ed.; CRC Press: Boca Raton, FL, 2014; pp 33−56. (r) Kimura, E.; Koike, T.; Aoki, S. Evolution of Zn^{II}-Macrocyclic Polyamines to Biological Probes and Supramolecular Assembly Elements. In *Macrocyclic and Supramolecular Chemistry: How Izatt-Christensen Award Winners Shaped the Field;* Izatt, R. M., Ed.; John Wiley & Sons, 2016; pp 417−445.

(7) (a) Gibb, C. L. D.; Gibb, B. C. Well-Defined, Organic Nanoenvironments in Water: The Hydrophobic Effect Drives a Capsular Assembly. *J. Am. Chem. Soc.* **2004**, *126*, 11408−11409. (b) Slagt, V. F.; Kamer, P. C. J.; van Leeuwen, P W. N. M.; Reek, J. N. H. Encapsulation of Transition Metal Catalysts by Ligand-Template Directed Assembly. *J. Am. Chem. Soc.* **2004**, *126*, 1526−1536. (c) Kuil, M.; Soltner, T.; van Leeuwen, P. W. N. M.; Reek, J. N. H. High-Precision Catalysts: Regioselective Hydroformylation of Internal Alkenes by Encapsulated Rhodium Complexes. *J. Am. Chem. Soc.* **2006**, *128*, 11344−11345. (d) Neelakandan, P. P.; Hariharan, M.; Ramaiah, D. A. Supramolecular Fluorescence Assay for Selective Recognition of GTP. *J. Am. Chem. Soc.* **2006**, *128*, 11334−11335. (e) Nishioka, Y.; Yamaguchi, T.; Yoshizawa, M.; Fujita, M. Unusual [2 + 4] and [2 + 2] Cycloadditions of Arenes in the Confined Cavity of Self-Assembled Cages. *J. Am. Chem. Soc.* **2007**, *129*, 7000−7001. (f) Natarajan, A.; Kaanumalle, L. S.; Jockusch, S.; Gibb, C. L. D.; Gibb, B. C.; Turro, N. J.; Ramamurthy, V. Controlling Photoreactions with Restricted Spaces and Weak Intermolecular Forces: Exquisite Selectivity during Oxidation of Olefins by Singlet Oxygen. *J. Am. Chem. Soc.* **2007**, *129*, 4132−4133. (g) Sawada, T.; Yoshizawa, M.; Sato, S.; Fujita, M. Minimal Nucleotide Duplex Formation in Water through Enclathration in Self-Assembled Hosts. *Nat. Chem.* **2009**, *1*, 53−56. (h) Gianneschi, N. C.; Nguyen, S. T.; Mirkin, C. A. Signal Amplification and Detection via a Supramolecular Allosteric Catalyst. *J. Am. Chem. Soc.* **2005**, *127*, 1644−1645. (i) Lee, S. J.; Cho, S.-H.; Mulfort, K. L.; Tiede, D. M.; Hupp, J. T.; Nguyen, S. T. Cavity-Tailored, Self-Sorting Supramolecular Catalytic Boxes for Selective Oxidation. *J. Am. Chem. Soc.* **2008**, *130*, 16828−16829. (j) Murase, T.; Horiuchi, S.; Fujita, M. Naphthalene DielsAlder in a Self-Assembled Molecular Flask. *J. Am. Chem. Soc.* **2010**, *132*, 2866−2867.

(8) (a) Merlau, M. L.; del Pilar Mejia, M.; Nguyen, S. T.; Hupp, J. T. Artificial Enzymes Formed through Directed Assembly of Molecular Square Encapsulated Epoxidation Catalysts. *Angew. Chem., Int. Ed.* **2001**, *40*, 4239−4242. (b) Yoshizawa, M.; Tamura, M.; Fujita, M. Diels-Alder in Aqueous Molecular Hosts: Unusual Regioselectivity and Efficient Catalysis. *Science* **2006**, *312*, 251−254. (c) Leung, D. H.; Bergman, R. G.; Raymond, K. N. Scope and Mechanism of the C-H Bond Activation Reactivity within a Supramolecular Host by an Iridium Guest: A Stepwise Ion Pair Guest Dissociation Mechanism. *J. Am. Chem. Soc.* **2006**, *128*, 9781−9797. (d) Leung, D. H.; Bergman, R. G.; Raymond, K. N. Highly Selective Supramolecular Catalyzed Allylic Alcohol Isomerization. *J. Am. Chem. Soc.* **2007**, *129*, 2746−2747. (e) Pluth, D. M.; Bergman, G. R.; Raymond, N. K. Acid Catalysis in Basic Solution: A Supramolecular Host Promotes Orthoformate Hydrolysis. *Science* **2007**, *316*, 85−88. (f) Iwasawa, T.; Hooley, R. J.; Rebek, J., Jr. Stabilization of Labile Carbonyl Addition Intermediates by a Synthetic Receptor. *Science* **2007**, *317*, 493−496. (g) Brown, C. J.; Bergman, R. G.; Raymond, K. N. Enantioselective Catalysis of the Aza-Cope Rearrangement by a Chiral Supramolecular Assembly. *J. Am. Chem. Soc.* **2009**, *131*, 17530−17531. (h) Pluth, M. D.; Bergman, R. G.; Raymond, K. N. The Acid Hydrolysis Mechanism of Acetals Catalyzed by a Supramolecular Assembly in Basic Solution. *J. Org. Chem.* **2009**, *74*, 58−63. (i) Shultz, A. M.; Farha, O. K.; Hupp, J. T.; Nguyen, S. T. A Catalytically Active, Permanently Microporous MOF with Metalloporphyrin Struts. *J. Am. Chem. Soc.* **2009**, *131*, 4204−4205. (j) Lee, J. Y.; Farha, O. K.; Roberts, J.; Scheidt, K. A.; Nguyen, S. T.; Hupp, J. T. Metal-Organic Framework Materials as Catalysts. *Chem. Soc. Rev.* **2009**, *38*, 1450−1459. (k) Pignataro, L.; Lynikaite, B.; Cvengros, J.; Marchini, M.; Piarulli, U.; Gennari, C. Combinations of Acidic and Basic Monodentate BinaphtholicPhosphites as Supramolecular Bidentate Ligands for Enantioselective Rh-Catalyzed Hydrogenations. *Eur. J. Org. Chem.* **2009**, *2009*, 2539−2547. (l) Hastings, C. J.; Pluth, M. D.; Bergman, R. G.; Raymond, K. N. Enzymelike Catalysis of the Nazarov Cyclization by Supramolecular Encapsulation. *J. Am. Chem. Soc.* **2010**, *132*, 6938−6940.

(9) Zulkefeli, M.; Hisamatsu, Y.; Suzuki, A.; Miyazawa, Y.; Shiro, M.; Aoki, S. Supramolecular Phosphatases Formed by the Self-Assembly of the Bis(Zn^{2+}-Cyclen) Complex, Copper(II), and Barbital Derivatives in Water. *Chem. - Asian J.* **2014**, *9*, 2831−2841.

(10) Hisamatsu, Y.; Miyazawa, Y.; Yoneda, K.; Miyauchi, M.; Zulkefeli, M.; Aoki, S. Supramolecular Complexes Formed by the Self-assembly of Hydrophobic Bis(Zn^{2+}-cyclen) Complexes, Copper, and Di- or Triimide Units for the Hydrolysis of Phosphate Mono- and Diesters in Two-Phase Solvent Systems (Cyclen = 1,4,7,10-Tetraazacyclododecane). *Chem. Pharm. Bull.* **2016**, *64*, 451−464.

(11) Sun, L.; Martin, D. C.; Kantrowitz, E. R. Rate-Determining Step of *Escherichia coli* Alkaline Phosphatase Altered by the Removal of a Positive Charge at the Active Center. *Biochemistry* **1999**, *38*, 2842−2848.

(12) Regarding this mechanistic hypothesis, the pH profile of MNP hydrolysis by the 4:4:4 supramolecular complex 30 formed by the self-assembly of **1** (Zn_2L^1), cyanuric acid, and Cu^{2+} in a single phase (water) is shown in Figure S1 of Supporting Information, based on which the reaction mechanism is proposed in Scheme S1 of Supporting Information. Further study on the reaction mechanism for the MNP hydrolysis by the supramolecular phosphatases is now underway.

(13) Kimura, E.; Aoki, S.; Koike, T.; Shiro, M. A Tris(Zn^{II}-1,4,7,10-tetraazacyclododecane) Complex as a New Receptor for Phosphate Dianion in Aqueous Solution. *J. Am. Chem. Soc.* **1997**, *119*, 3068−3076.

DOI: 10.1021/acs.inorgchem.8b03586
Inorg. Chem. XXXX, XXX, XXX−XXX

(14) De León-Rodríguez, L. M.; Kovacs, Z.; Esqueda-Oliva, A. C.; Miranda-Olvera, A. D. Highly Regioselective *N*-trans Symmetrical Diprotection of Cyclen. *Tetrahedron Lett.* **2006**, *47*, 6937−6940.

(15) Schubert, U. S.; Eschbaumer, C.; Hochwimmer, G. High Yield Synthesis of 5,5′-Dimethyl-2, 2′-bipyridine and 5,5′′-Dimethyl-2,2′:6′,2′′-terpyridine and Some Bisfunctionalization Reactions Using *N*-Bromosuccinimide. *Synthesis* **1999**, 779−782.

(16) Aoki, S.; Zulkefeli, M.; Shiro, M.; Kohsako, M.; Takeda, K.; Kimura, E. A Luminescence Sensor of Inositol 1, 4,5-Triphosphate and Its Model Compound by Ruthenium-Templated Assembly of a Bis(Zn^{2+}-Cyclen) Complex Having a 2, 2'-Bipyridyl Linker (Cyclen = 1, 4,7, 10-Tetraazacyclododecane). *J. Am. Chem. Soc.* **2005**, *127*, 9129−9139.

(17) Gaunt, M. J.; Yu, J.; Spencer, J. B. Rational Design of Benzyl-Type Protecting Groups Allows Sequential Deprotection of Hydroxyl Groups by Catalytic Hydrogenolysis. *J. Org. Chem.* **1998**, *63*, 4172−4173.

(18) (a) Carreira-Barral, I.; Mato-Iglesias, M.; de Blas, A.; Platas-Iglesias, C.; Tasker, P. A.; Esteban-Gómez, D. Ditopic Receptors Containing Urea Groups for Solvent Extraction of Cu(II) Salts. *Dalton Trans.* **2017**, *46*, 3192−3206. (b) Carreira-Barral, I.; Fernández-Pérez, I.; Mato-Iglesias, M.; de Blas, A.; Platas-Iglesias, C.; Esteban-Gómez, D. Recognition of AMP, ADP and ATP through Cooperative Binding by Cu(II) and Zn(II) Complexes Containing Urea and/or Phenylboronic Acid Moieties. *Molecules* **2018**, *23*, 479. (l) Mesquita, L. M.; Mateus, P.; Fernandes, R. D. V.; Iranzo, O.; André, V.; Tiago de Oliveira, F.; Platas-Iglesias, C.; Delgado, R. Recognition of Phosphopeptides by a DinuclearCopper(II) Macrocyclic Complex in a Water: Methanol 50:50 v/v Solution; *Dalton Trans.* **2017**, *46*, 9549−9564.

(19) Sagel, I. H. *Biochemical Calculations,* 2nd ed.; John Wiley & Sons: New York, 1976; pp 246−272.

(20) Negligible effect of F^- (NaF) on the MNP hydrolysis by **10** was observed.

(21) The quantum yields for the emission of bpy in H_2O and $CHCl_3$ (excitation at 293 nm) were determined to be 5.6×10^{-3} and 6.2×10^{-3}, respectively, by comparison with the integrated correlated emission spectrum of quinine sulfate standard, whose emission quantum yield in 0.1 M H_2SO_4 was 0.55 (excitation at 366 nm).

(22) (a) Qian, G.; Wang, M. Excimer Luminescence of 2, 2 Bipyridine in the Silica Gel Glass. *Mater. Lett.* **2002**, *56*, 71−75. (b) Klessinger, M.; Michl, J. *Excited States and Photochemistry of Organic Molecules;* VCH Publishers: New York, 1995; pp 278−281.

(23) The emission quantum yield of **1** in H_2O was determined to be 2.5×10^{-3} (excitation at 293 nm) by comparison with the integrated correlated emission spectrum of quinine sulfate standard, as described in ref 21.

(24) (a) Starks, C. M.; Liotta, C. L.; Halpern, M. *Phase-Transfer Catalysis: Fundamentals, Applications, and Industrial Perspectives;* Chapman and Hall: New York, 1994. (b) Donnell, M. J. Asymmetric Phase Transfer Reactions. In *Catalytic Asymmetric Synthesis;* Ojima, I., Ed.; VCH: New York, 1993; pp 389−411. (c) Maruoka, K. *Asymmetric Phase Transfer Catalysis;* Wiley-VCH Verlag GmbH & Co.: Weinheim, Germany, 2008.

DOI: 10.1021/acs.inorgchem.8b03586
Inorg. Chem. XXXX, XXX, XXX−XXX